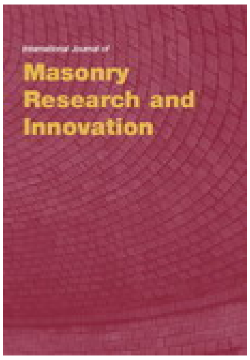

International Journal of Masonry Research and Innovation

ISSN online: 2056-9467 - ISSN print: 2056-9459
https://www.inderscience.com/ijmri

Comparison of simplified coupled and uncoupled 3D finite element models for soil-structure interactions in masonry structures with strip foundations undergoing subsidence

Alfonso Prosperi, Michele Longo, Paul A. Korswagen, Mandy Korff, Jan G. Rots

DOI: 10.1504/IJMRI.2025.10070775

Article History:

Received:	15 October 2024
Last revised:	06 February 2025
Accepted:	12 February 2025
Published online:	06 May 2025

Comparison of simplified coupled and uncoupled 3D finite element models for soil-structure interactions in masonry structures with strip foundations undergoing subsidence

Alfonso Prosperi*, Michele Longo and Paul A. Korswagen

Faculty of Civil Engineering and Geosciences,
Delft University of Technology,
Stevinweg 1, 2628 CN, The Netherlands
Email: a.prosperi@tudelft.nl
Email: M.Longo@tudelft.nl
Email: p.a.korswageneguren@tudelft.nl
*Corresponding author

Mandy Korff

Faculty of Civil Engineering and Geosciences,
Delft University of Technology,
Stevinweg 1, 2628 CN, The Netherlands
and
Deltares,
P.O. Box, 177, 2600 MH Delft, The Netherlands
Email: M.Korff@tudelft.nl

Jan G. Rots

Faculty of Civil Engineering and Geosciences,
Delft University of Technology,
Stevinweg 1, 2628 CN, The Netherlands
Email: J.G.Rots@tudelft.nl

Abstract: This study compares two 3D nonlinear FE models, 'simplified coupled' and 'uncoupled', to explore 'light' damage in a two-storey masonry building on strip foundations affected by subsidence. Both models employ nonlinear interfaces to simulate soil-structure interaction: the simplified coupled model ties the structure with the soil volume with 'contact interfaces', while the uncoupled model uses 'boundary interfaces' to represent the interaction. The impact of soil volume and settlement shape size is examined. Results indicate consistent damage, displacements, and stresses across both modelling approaches with the smallest soil volume. Differences increase with larger soil volumes: at a distortion of 1/1,000 in hogging, the coupled model shows the damage decreases by 54% when the soil volume is quadrupled. Mesh size is also observed to affect crack initiation but not the overall damage mechanism. In general, coupled models reduce non-convergence and computation time, whereas uncoupled models simplify the analyses by decoupling the problem.

Keywords: masonry; damage; settlements; numerical models; soil-structure interaction; 3D FE analyses; subsidence; soil-foundation interfaces; strip foundations; cracking.

Reference to this paper should be made as follows: Prosperi, A., Longo, M., Korswagen, P.A., Korff, M. and Rots, J.G. (2025) 'Comparison of simplified coupled and uncoupled 3D finite element models for soil-structure interactions in masonry structures with strip foundations undergoing subsidence', *Int. J. Masonry Research and Innovation*, Vol. 10, No. 7, pp.1–41.

Biographical notes: Alfonso Prosperi is a Postdoctoral Researcher at Delft University of Technology (TU Delft). His research interests encompass the effects of settlement on structures, soil–structure interactions, and the assessment of damage in masonry buildings.

Michele Longo is a Civil Engineering graduate from the University of Parma, Italy. He completed his MSc thesis at TU Delft in 2016. Since 2017, he has been working on sensitivity studies of unreinforced masonry structures, focusing on both serviceability and ultimate limit states.

Paul A. Korswagen is an Assistant Professor in the section of Applied Mechanics at the faculty of Civil Engineering and Geosciences of TU Delft. His research focuses on the risk analysis of building damage from multiple hazards, such as earthquakes, floods and settlements.

Mandy Korff is an Associate Professor (TU Delft) in Geotechnical Practice (since 2016) and Senior Advisor at Deltares. Her expertise spans underground construction, soil-structure interaction, forensic geo-engineering, and risk management.

Jan G. Rots is a full professor of Structural Mechanics at the faculty of Civil Engineering and Geosciences of TU Delft. He concentrates on the principles of strength, distortions and tensions and their effect on buildings.

This paper is a revised and expanded version of a paper entitled 'Comparative analysis of coupled and uncoupled 3D finite elements models for masonry structures subjected to settlements' presented at 18th International Brick and Block Masonry Conference, IB2MaC 2024, University of Birmingham, Edgbaston Park Hotel, Birmingham, UK, 21–24 July 2024.

1 Introduction

Land subsidence triggered by a combination of natural and anthropogenic drivers causes the progressive lowering of the ground surface relative to the sea level. Moreover, the rates of land subsidence are evolving, as the process is influenced by the more intense and frequent droughts and rains due to climate change.

At the scale of single structures, land subsidence is responsible for the occurrence of differential settlements, which can cause deformation and damage to existing buildings. This issue is particularly relevant for existing unreinforced masonry buildings, ubiquitous in the Netherlands, which are characterised by the low tensile properties of the masonry material. Although some buildings rely on piled foundations, which reach deep and stable soil layers, estimates reveal that 70% of buildings rest on shallow foundation systems (i.e., rafts, strips) and are thus directly exposed to (surface) ground movements.

While differential settlements can result in severe structural damage and even cause partial or total building collapse, masonry structures in the Netherlands more commonly exhibit 'light' damage, typically associated with minor aesthetic and functional issues. In this context, predictions are essential for assessing the behaviour of exposed masonry structures and, consequently, for identifying areas where buildings may be particularly vulnerable.

Numerical simulations offer a valuable method for examining the structural behaviour of specific building types, especially when empirical observations are limited to a few cases or are not available (Dalgic et al., 2019; Son and Cording, 2005). Additionally, numerical models help address the gap caused by the limited availability of experimental tests in the scientific literature, where only a few examples are available, for instance, in Giardina et al. (2012) and Dalgic et al. (2023).

Earlier studies (e.g., Prosperi et al., 2023b; Korswagen et al., 2023) focus on modelling structures affected by subsidence and examine how various structural features influence building responses. These studies demonstrated how the nonlinear damage response of the structures, in terms of cracking damage, can be correlated with the subsidence, as measured by the soil angular distortions (β). Moreover, these studies corroborate that the results of the models depend on the soil-structure interaction and the methods employed to integrate it, as confirmed by the state-of-the-art.

Different modelling approaches can be employed to simulate the soil-structure interaction in structures undergoing settlements:

- *Coupled models* (Giardina et al., 2013; El Naggar et al., 2020; Burd et al., 2022), where the soil, structure and foundation are integrated into a single model. Within the soil model, the settlement driver is included, and the mutual interaction between the settlement driver, the soil and the structural system is accounted for [also defined as 'fully-coupled models' (Giardina et al., 2013a; Burd et al., 2000, 2022; Ninić et al., 2024; Bilotta, 2017)]. In contrast, when the settlement is applied at the boundary of the model and the soil block primarily serves as an intermediate layer between the input and the structure, these are referred herein to as 'simplified coupled models' (Son and Cording, 2005).

- *Uncoupled models* (Giardina et al., 2013a; Burd et al., 2000, 2022; Ninić et al., 2024; Bilotta, 2017; Bilotta et al., 2017; Lin et al., 2020), two separate models are used for the soil and the structure. Uncoupled models can be further categorised into *decoupled models*, where soil displacements are directly applied to the structural model without accounting for the soil-structure interaction, and *semi-coupled models*, where displacements are applied at the base of an interface accounting for the soil-structure interaction.

This study compares two modelling approaches, i.e., simplified coupled models and uncoupled (semi-coupled) analyses, to represent the soil-structure interaction and to assess the response of masonry structures on strip foundations subjected to subsidence-related settlements. The aim is to investigate how the choice of modelling strategy and soil-structure interaction affects the results. The performance and differences between the two approaches are compared to understand their impact on the outcomes.

This paper starts with Section 2, presenting the methodology and finite element models. Section 3 covers the results, Section 4 discusses the findings, and Section 5 summarises the main conclusions.

2 Methodology and finite element models

2.1 Methodology

In this study, two 3D modelling techniques are used to simulate the response of structures undergoing subsidence. The aim is to compare their performance and results in terms of displacements, damage and stresses, and to assess their differences.

Figure 1 Flowchart of the different phases of the analysis of this study (see online version for colours)

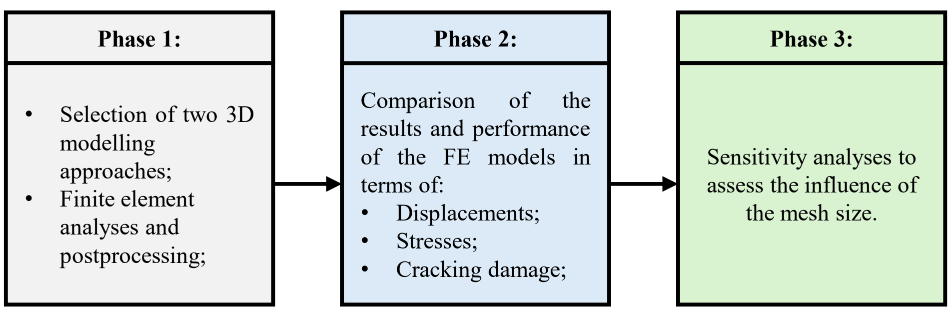

Accordingly, a three steps approach is followed (Figure 1):

- In *phase 1*, 3D finite element models are built. The analyses are carried out, and the results are post-processed to prepare them for comparison.
- In *phase 2*, the results of the finite element analyses are compared in terms of displacements, stresses, crack patterns, and damage severity. Additionally, the characteristics of the numerical analyses, such as the number of elements and nodes and the convergence of the iterative procedure, are examined. The models that exhibit the best agreement are chosen for further sensitivity analyses.
- In *phase 3*, sensitivity analyses are conducted to assess the impact of mesh size on the numerical results.

2.2 Selected modelling approaches

This study focuses on 3D nonlinear models for masonry buildings subjected to subsidence. In scientific literature, finite element simulations are commonly employed to model the structural responses to settlements caused by tunnelling, mining, and excavations. However, other factors like groundwater lowering, organic soil oxidation, or clay shrinkage can also induce surface ground movements. This is particularly relevant in urban areas prone to subsidence, such as regions in the western and northern Netherlands, where multiple drivers often overlap. Accurately incorporating all overlapping factors and their interactions with soil and structures is often impractical. Consequently, the chosen modelling strategies exclude the settlement driver from the model, directly accounting for its effect in terms of displacements, thereby reducing both the modelling burden and complexity.

The two modelling 3D approaches, are used for the analyses carried out with the finite element method software Diana FEA 10.7 and they are schematically illustrated in Figure 2:

- The 'simplified coupled' model [Figure 2(a)] consists of a 3D model with shell elements of the building and strip foundation, without floors and party walls. The model is based on the work of Son and Cording (2005), Giardina et al. (2013), Burd et al. (2000, 2022), Netzel and Kaalberg (2000) and Yiu et al. (2017) and closely follows the modelling approach outlined in Son and Cording (2005). While a fully coupled model would account for the complex interactions between the soil, foundation, structure, and settlement driver, modelling the effects of multiple sources of settlement drivers within the soil may be unfeasible. Therefore, a simplified approach is herein adopted: a linear-elastic soil layer is included and tied to the structural model using contact interface elements. However, this soil layer is not intended to accurately capture the actual behaviour of the soil beneath the building. The key idea of this approach is that the combination of the dummy soil layer and contact interfaces can represent the effect of soil-structure interaction with the superficial soil layer, while the settlement driver affects the deeper strata. Settlements are thus applied as imposed displacements at the bottom of the soil stratum.
- The 'uncoupled' model [Figure 2(b)], consists of two sub-systems that separate the soil and the superstructure: the soil sub-system [Figure 2(b.0)] mirrors the dummy elastic soil in the simplified coupled model, allowing for consistent comparison, as it has been initially hypothesised that the soil volume could slightly decrease the distortion of the applied displacement fields transmitted to the structure. The uncoupled model features two steps: In step 1, as in the simplified coupled model, settlements are applied as displacements at the base of the soil layer. The displacements from the top of the soil are then used as input for the structural model in step 2 [Figure 2(b.1)], which shares the same features as the structural subsystem of the simplified coupled model [Figure 2(a)]. The main distinction is the boundary interfaces adopted in the structural subsystem of the uncoupled approach, representing the soil-structure interaction. The structural subsystem with boundary interfaces has been adopted in previous studies (e.g., Dalgic et al., 2019; Prosperi et al., 2023b; Longo et al., 2021; Drougkas et al., 2020; Ferlisi et al., 2020).

Thus, the main difference between the two selected modelling approaches lies in the representation of the soil-structure interaction. The same settlement profiles, detailed in the following, are imposed in both modelling approaches.

Figure 2 The selected 3D modelling approaches, (a) the simplified coupled model consisting of a soil volume tied to the superstructure via nonlinear contact interfaces and (b) the uncoupled model, including (b0) the soil model imposed and (b1) the structural model (see online version for colours)

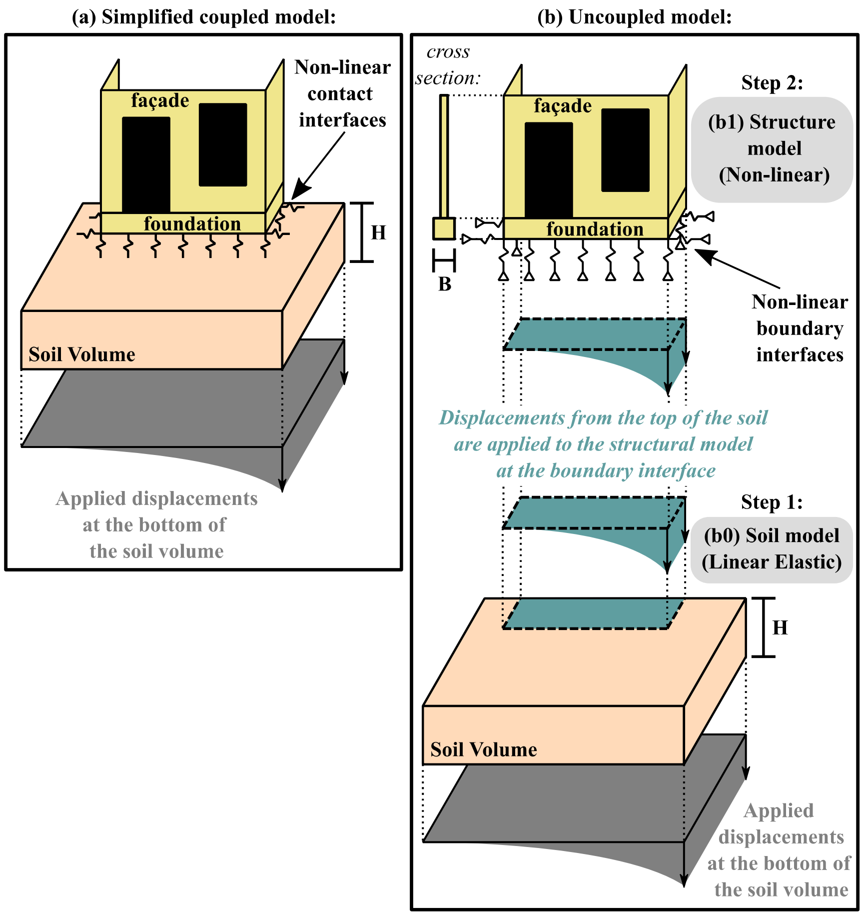

(a) (b)

Notes: Settlements are applied as imposed displacements at the bottom of the soil volume in both models. In the uncoupled approach, the displacements retrieved at the top of the soil volume are then applied to the structural model at the bottom of the boundary inferences.

2.3 *Geometry and FEM discretisation*

2.3.1 *Superstructure*

The selected case study corresponds to a two-storey masonry building, already considered in previous studies (Prosperi et al., 2023b, 2024), representing typical old Dutch houses (Jafari, 2021) [such as in Figure 3(a)]. The façade of the building is 8 metres wide and 7 metres tall, consisting of a single-wythe wall with a thickness of 0.1 metres. The lateral walls in the model match the façade’s height. The inclusion of lateral house-to-house separation walls has been found to affect the structural response to settlements (Prosperi et al., 2024). To simplify the models, symmetry is applied, so only half of the transversal wall, with a length equal to half of the façade, is represented [Figure 3(b)].

Figure 3 (a) An example of a historical masonry building located in Delft, the Netherlands, photographed by Wikipedia (2010) and (b) the structural finite element models adopted in this study for both simplified coupled and uncoupled models (see online version for colours)

(a) – Monument ID: 11994

(b) – The equivalent finite element model

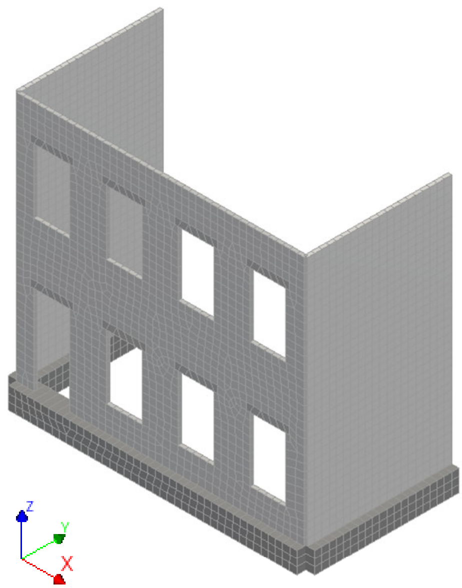

The models include the masonry strip foundation system below the walls, commonly observed in such old buildings, with a rectangular cross-section characterised by a base 'B' (perpendicular to the façade) measuring 500 millimetres and a height of 600 millimetres. Masonry lintels above openings are included. The lintels, strip foundation, and walls are discretised using quadrilateral (8-node) and triangular (6-node) shell elements, with an average mesh size of 200 × 200 millimetres. A 3 × 3 Gauss integration scheme is applied in the plane of the elements, while five integration points, based on Simpson's rule, are used for the thickness of the shell elements.

The structural models aim to represent the behaviour of old Dutch masonry buildings with timber roofs and floors. However, these timber elements were not included in the models, as they have been observed to have minimal impact on the structural response when subjected to subsidence (Prosperi et al., 2024).

2.3.2 Soil volume

The soil volume used in the analyses was assumed to have a height 'H' of 600 mm, which is 1.2 times the foundation base 'B'. This value was chosen as an initial estimate, based on the depth of the pressure bulbs for the strip foundation derived from the

Boussinesq equation (Bowles, 1988). Specifically, the depth of the pressure bulb corresponding to 50% of the applied surface load is considered, which is approximately 1.2 times ‘B’. Since the soil height ‘H’ is hypothesised to affect the results, two additional soil heights, 1,200 mm and 2,400 mm or 2 and 4 times the initial estimate respectively, were considered to further assess its influence.

The boundaries of the soil volume are positioned 8 meters away from the walls, resulting in a soil volume of 24 m × 12 m x ‘H’, which is discretised using brick (20-node) and wedge (15-node) elements. The mesh size of the soil near the building, within 2 meters of it, ranges from 200 mm to 400 mm, while the mesh size for the rest of the soil elements ranges from 400 mm to 800 mm. A 2 × 2 × 2 Gauss integration scheme is applied to the soil volume.

2.4 Material properties

The structural models include clay-baked masonry for the façade, transverse walls, lintels, and strip foundations. The nonlinear cracking behaviour of the masonry material was modelled using an orthotropic smeared crack/shear/crush constitutive law, specifically the Engineering Masonry Model (EMM) (Schreppers et al., 2016; Rots et al., 2016). Therefore, the masonry material is not modelled distinguishing the units, bed- and head-joints, but as a homogenised orthotropic smeared model. Moreover, the EMM requires the specification of the angle at which stair-case cracks will initiate and propagate diagonally in the masonry, depending on the masonry pattern.

Table 1 Material properties of the baked-clay masonry adopted in the FE models

Material properties	*Symbol*	*Unit of measure*	*Value*
Young’s modulus vertical direction	E_y	[MPa]	5,000
Young’s modulus horizontal direction	E_x	[MPa]	2,500
Shear modulus	G_{xy}	[MPa]	2,000
Bed joint tensile strength	f_{ty}	[MPa]	0.10
Minimum head-joint strength	$f_{tx,min}$	[MPa]	0.15
Fracture energy in tension	$G_{ft,I}$	[N/mm]	0.01
The angle between stepped crack and bed-joint	α	[rad]	0.50
Compressive strength	f_c	[MPa]	8.50
Fracture energy in compression	G_c	[N/mm]	20.00
Friction angle	φ	[rad]	0.70
Cohesion	c	[MPa]	0.15
Fracture energy in shear	G_s	[N/mm]	0.10
Mass density	ρ	[Kg/m^3]	1708

Note: The Y direction corresponds to the vertical axis, perpendicular to the bed joints.

Source: Schreppers et al. (2016), NPR9998:2020en (2021) and Korswagen et al. (2017)

The material properties for the selected fired clay brick masonry (Table 1) were obtained from the literature and the Dutch standard (Schreppers et al., 2016; NPR9998:2020en, 2021; Korswagen et al., 2017). In finite element analyses, the crack bandwidth is determined using Govindjee’s projection method, which takes into account not only the finite element size but also its aspect ratio and the crack orientation (Govindjee et al., 1995).

For the soil volume, the analyses use a Young's modulus of 29 MPa, a shear modulus of 10 MPa, and a Poisson's ratio of 0.45. The selected soil is also characterised by a friction angle of 0.29 radians (approximately 17°) and no cohesion. Additionally, the soil block is assigned a mass of 2,000 kg/m^3 and a K_0 value of 0.5. The soil properties are subsequently used to define the stiffness values of the interface elements or to assign them directly to the soil volume.

2.5 Soil-foundation interaction and interface elements

Both simplified coupled and uncoupled (semi-coupled) modelling approaches use nonlinear interfaces to represent the soil-foundation interaction. The interface elements relate the forces acting on the interface to the relative displacement between its two sides (DIANA FEA, 2023).

In the case of the simplified coupled models, the superstructure is tied with the soil volume using interface elements [Figure 4(a)]. This type of interface element is herein referred to as 'contact interface', to distinguish it from the one adopted in the uncoupled models.

Figure 4 Schematic illustration of the adopted interface typologies, (a) contact interfaces and (b) boundary interfaces (see online version for colours)

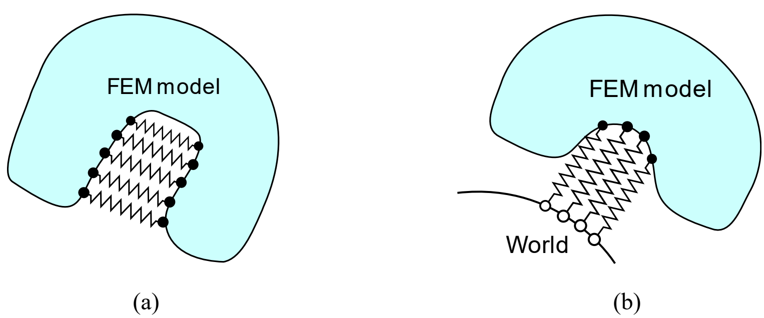

Source: Images retrieved from DIANA FEA (2023)

Table 2 Values of the vertical and tangential interface stiffness of the adopted models (for a mesh size of 200 × 200 millimetres)

Interface type	*Parameter*	*Value [N/mm^3]*
Contact interface	K_n	2.22E-01
	K_t	2.02E-02
Boundary interface	K_n	3.35E-02
	K_n (foundation corners)	4.10E-02
	K_t	2.26E-02

In contrast, the uncoupled approach treats the superstructure and soil volume as separate subsystems. The boundary interface elements [Figure 4(b)] adopted in the uncoupled analyses must not only allow the transmission of stresses and displacements but also represent the behaviour, in terms of stiffness, of the soil volume which is not tied to the superstructure.

The following subsections describe two different analytical formulations for computing the stiffness of the selected types of interfaces. Both coupled and uncoupled analyses employ the Coulomb-friction constitutive law with no tensile strength for the interfaces. The normal and shear stiffness of the interfaces are defined by the geotechnical properties of the selected soil.

2.5.1 Contact interfaces

The normal and tangential stiffnesses at the contact interface [Figure 4(a)] are calculated using equations (1) and (2) provided by DIANA FEA (2023). This analytical approach computes the values of the normal and shear stiffness of the interfaces placed between structural elements and the soil using the properties of the adjacent soil (DIANA FEA, 2023).

$$K_n = \left(\frac{2}{3}\right)^2 \frac{E}{2(1+v)\dfrac{l_{interface}}{10}} \tag{1}$$

$$K_t = \frac{K_n}{11} \tag{2}$$

where E represents the Young's modulus of the adjacent soil, and v is the Poisson's ratio. $l_{interface}$ denotes the length of the individual interface element, which is dependent on the mesh size (DIANA FEA, 2023). The division of $l_{interface}$ by 10 is based on the assumption that the virtual thickness of the interface is 0.1 times the length of the element. The computed values are reported in Table 2.

2.5.2 Boundary interfaces

The boundary interface [Figure 4(b)] normal and tangential stiffnesses are computed using the equations provided by NEHRP (2012), Gazetas (1991) and Mylonakis et al. (2006), for arbitrarily shaped foundations on a homogeneous half-space (Ferlisi et al., 2020):

$$K_n = \frac{GL}{1-v}\left[0.73 + 1.54\left(\frac{B}{L}\right)^{0.75}\right] \tag{3}$$

$$K_t = GL\left[\frac{1}{2-v}\left[2 + 2.5\left(\frac{B}{L}\right)^{0.85}\right] - \frac{0.2}{2(0.75-v)}\left[1 - \frac{B}{L}\right]\right] \tag{4}$$

where K_n, and K_t in equations (3) and (4) represent the static stiffnesses for a rigid foundation for the normal, and tangential (i.e., in the plane of the façade) directions to the soil surface. G denotes the soil shear modulus, B represents the foundation base (i.e., perpendicularly to the façade), and L is the foundation length (equal to the length of the façade). Since the vertical soil stiffness is not uniform and tends to increase near the corners of the foundation K_n is increased by a coefficient R_k which consider the increase in the spring stiffness, as reported in NEHRP (2012). The computed value of R_k is slightly above 1.2 in this application. The values of K_n multiplied by R_k and applied to both sides of the façade over a length equal to 1/6 of its total length. The values of K_n, and K_t are then divided by B and L to obtain smeared values of the normal and shear linear stiffness. These computed values are reported in Table 2. The normal interface stiffness value computed for boundary interfaces is approximately 5.41 times smaller than the value computed for contact interfaces. This difference can be attributed to the fact that boundary interfaces account not only for the behaviour at the contact surface between the foundation and the adjacent soil but also for the behaviour of the surrounding soil, which is not represented in the structural model.

The equations proposed by Gazetas (1991) have been already used in previous studies to compute the normal and tangential stiffness for structures undergoing settlements (Drougkas et al., 2020; Ferlisi et al., 2019). In Drougkas et al. (2020) and Ferlisi et al. (2019), the stiffness values were calculated based on the properties of the soil directly supporting the structure, and this same approach is used here.

2.6 Boundary restrains

In both modelling approaches, only half of the building is modelled. Symmetric boundary conditions are applied to the edges of the transversal walls and transversal strip foundations, restricting in-plane translation and rotation about the vertical axis. For the uncoupled model, vertical and horizontal translational supports are provided at the bottom of the boundary interface. Translational supports in the normal direction are applied at both the bottom and on all four sides of the soil volume. After the gravity loads are applied, the supports on the four lateral sides are removed. This step enables the soil volume to move horizontally as well.

2.7 Gravity and settlement loads

Both the simplified coupled and the uncoupled models are subjected to gravity loads and settlement actions.

Two asymmetric settlement profiles are imposed at the base of the soil volume, artificially representing the effects of subsidence processes occurring in deeper soil layers not included in the models. In other words, the imposed settlements are not driven by any specific mechanism modelled within the soil but are instead an idealised representation. These settlement shapes, conformed to a Gaussian curve and based on data from the literature (Charles and Skinner, 2004; Prosperi et al., 2023a; De Vent, 2011), simulating the loss of support caused by settlements without causing the soil to unrealistically pull on the foundations (Prosperi et al., 2023b).

The settlement shapes are imposed at the bottom of the soil volume as input displacements and are computed using equation (5):

$$S(x) = S_{\max}\left\{(-1)^{\iota}\left(e^{\left[\frac{-(x-D_x)^2}{2x_i^2}\right]}\right)\right\} \tag{5}$$

where

- 'D_x' is the horizontal distance between the symmetry axis of the Gaussian curve and the edge of the building;

- 'x_i' is the distance from the symmetry axis of the curve to the point of inflexion;
- '$\imath$' is a term that enables controlling the convexity of the Gaussian curve.

The two settlement shapes are obtained by arbitrarily imposing the parameters D_x and x_i equal to 1.0 × L and 0.25 × L, respectively, with the parameter $\imath$ being set to 1 for the 'hogging' case [Figure 5(a)] and 0 for 'sagging' [Figure 5(b)].

Figure 5 Schematic illustration of the location of the different displacements in the models and settlement profiles applied in the finite element models, (a) hogging and (b) sagging (see online version for colours)

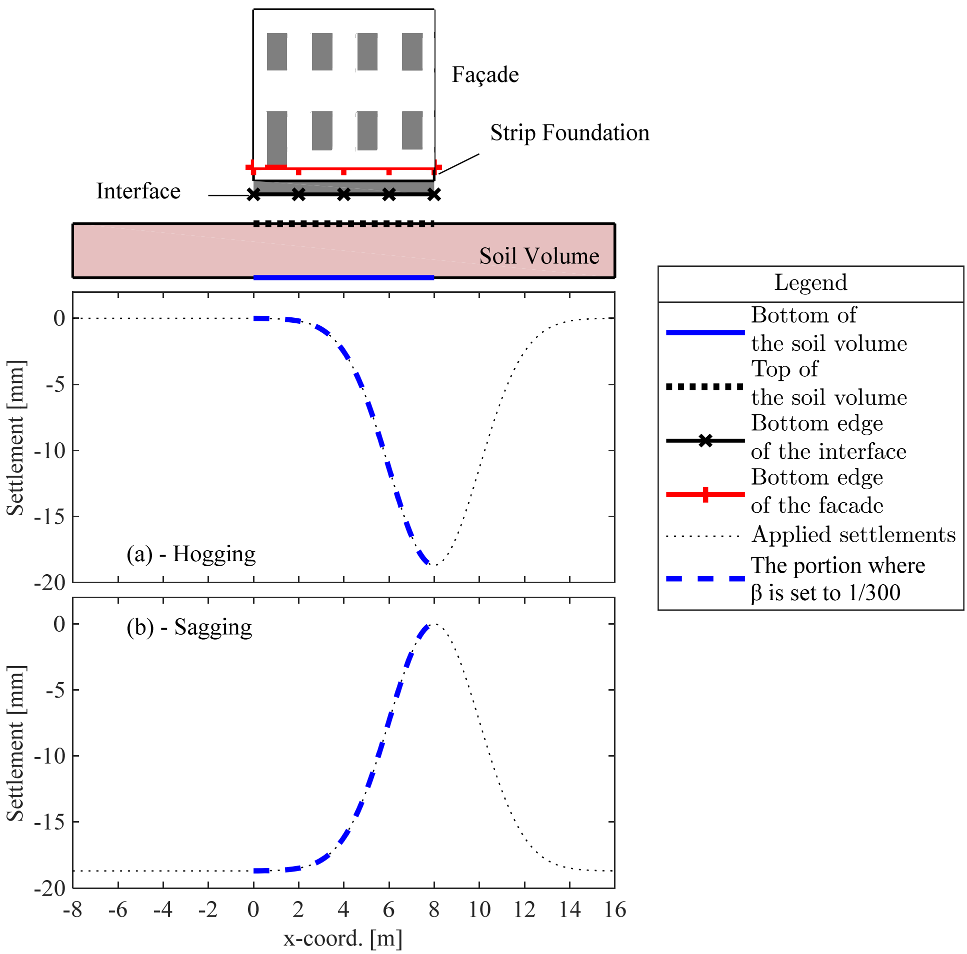

The amplitude of the settlement patterns, specifically the maximum settlement, is adjusted using the scalar S_{max} to ensure that the angular distortion (β) imposed at the base of the soil volume beneath the building (Figure 5) is equal to 1/300. The chosen values for the maximum angular distortion are 1.5 times higher than the acceptable value specified in Eurocode 7 for structures, which is 1/500 (CEN, 2004). Eurocode 7 also states that "The maximum acceptable relative rotations for open framed structures, infilled frames and load bearing or continuous brick walls are unlikely to be the same but are likely to range from about 1/2,000 to about 1/300, to prevent the occurrence of a serviceability limit state in the structure" (CEN, 2004). The imposed angular distortion represents the maximum value along the line which results from the projection of the façade's base at the bottom of the soil volume.

Depending on the type of model, a different procedure is adopted to apply the loads:

- In the simplified coupled model, a three-phase load application procedure is implemented: first, the K_0 procedure is carried out for the soil volume. The K_0 procedure is employed to determine the initial stress state in the soil based on the lateral pressure ratio, K_0. This ratio is defined as the horizontal effective stress divided by the vertical effective stress. In this case, the specified K_0 ratio is 0.5. Next, the structure is introduced, and its self-weight is applied in a single step to determine the initial stress state. The displacements are reset to zero after the application of gravity loads. Finally, the settlement profiles are applied in 374 steps, with a load rate of 0.05 mm per step.
- In the uncoupled model, the equivalent of the first phase in the coupled model is performed using a separate soil model [Figure 2(b.0)]. The same settings as in the simplified coupled model are then applied for the gravity and settlement loads.

In both modelling approaches, the weight (and stiffness) of the timber roof and timber are neglected on the basis that they are unlikely to contribute significantly to the behaviour of the building (Yiu et al., 2017; Prosperi et al., 2024).

The iterative method used during the application of settlements in both the simplified coupled and uncoupled models is the secant (quasi-Newton) method. Convergence is achieved when both force and displacement norms are simultaneously satisfied, with a tolerance level set at 1%. In case of non-convergent step, the analysis is set to 'Continue'. The line-search option is activated to stabilise the convergence process and improve convergence speed (DIANA FEA, 2023). The maximum number of iterations allowed per step is set to 75.

2.8 Assessment of the cracking damage

The numerical analyses carried out with the software Diana FEA produce tabulated outputs which summarise the information of the crack width in the principal direction at each integration point of the finite element mesh. These data are then used to quantify the damage in each step of the analyses, and thus the damage progression and accumulation during the progression of the imposed settlement.

The damage parameter Ψ (Korswagen et al., 2019) computed by means of (6), considering the number of cracks, their length and opening, is used to objectively assess the damage:

$$\Psi = 2n_c^{0.15}\hat{c}_w^{0.3} \tag{6}$$

where 'n_c' is the number of cracks, '$\hat{c}_w$' is the width-weighted and length-averaged crack width (in millimetres), computed with equation (7):

$$\hat{c}_w = \frac{\sum_{i=1}^{n_c} c_{w,i}^2 c_{L,i}}{\sum_{i=1}^{n_c} c_{w,i} c_{L,i}} \tag{7}$$

where '$c_{w,i}$' is the maximum crack width along the *i*-crack in mm, while '$c_{L,i}$' is the *i*-crack length in millimetres. A MATLAB script is used to compute the values of Ψ for each step of the numerical analyses. The computed Ψ values are then related to the damage severity categorised according to the system proposed by Burland and Wroth (1975) and shown in Table 3.

Table 3 Damage scale with the classification of visible damage and the corresponding discretisation of the damage parameter in sub-levels

Damage level	*Degree of damage*	*Approximate crack width*	*Parameter of damage*
DL0	No damage	Imperceptible cracks	$\Psi < 1$
DL1	Negligible	Up to 0.1 mm	$1 \leq \Psi < 1.5$
DL2	Very slight	Up to 1 mm	$1.5 \leq \Psi < 2.5$
DL3	Slight	Up to 5 mm	$2.5 \leq \Psi < 3.5$

Source: From Korswagen et al. (2019), Burland et al. (1979) and Grünthal (1998)

It is important to note that the parameter Ψ was proposed to examine the onset and progression of light damage, specifically cracking with a width of up to 5 millimetres ('DL3' in Table 3) (Korswagen et al., 2019). This research focuses on this particular type of damage caused by settlements in masonry structures. Cracking beyond this range, which could lead to a notable reduction in structural capacity, is not the focus of this study and would be more appropriately assessed using different metrics.

3 Results

3.1 Displacements during the application of the settlements

This study distinguishes the displacements retrieved at different locations in the numerical models (see Figure 5):

- The displacements imposed at the bottom of the soil block (input).
- Those retrieved at the bottom of the soil-foundation interfaces.
- Those retrieved at the bottom of the masonry façade, i.e., the top edge of the strip foundation.

Figure 6 and Figure 7 show the displacements obtained from the two models at the end of the application of the hogging and sagging settlement displacements respectively. Both figures show the results for an imposed angular distortion of 1/300, marking the end of the settlement phase, and for varying soil heights.

In both the hogging and sagging cases (Figure 6 and Figure 7 respectively) differences are observed between the input displacements (imposed at the bottom of the soil volume), the displacements measured at the bottom of the soil-foundation interface, and those at the base of the façade. For coupled models, the distortions imposed at the bottom of the soil volume are reduced already at the bottom of the interface, with this reduction becoming more pronounced as the soil height increases from 600 mm to 2,400 mm. This shows that the displacements at the bottom of the interface are influenced by the superstructure tied to the soil block, and there are thus only negligible differences between the displacements at the interface and those at the bottom of the façade for coupled models.

In contrast, for the uncoupled models, the displacements at the bottom of the interface show negligible differences compared to those imposed at the bottom of the soil block. The reduction of distortion played by the elastic soil block is negligible, though it becomes slightly more noticeable as the soil height increases. A reduction in distortion is seen between the displacements retrieved at the interface and those at the base of the façade, suggesting that in the uncoupled model, the imposed distortions are reduced when the displacements are transferred from the soil-foundation interface to the superstructure.

Figure 6 Vertical displacements retrieved for the coupled and uncoupled models in hogging at the last step of the numerical analysis (step 374 with applied angular distortion equal to 1/300) soil height of 600 mm for (a) and (b), 1,200 mm for (c) and (d), 2,400 mm for (e) and (f) (see online version for colours)

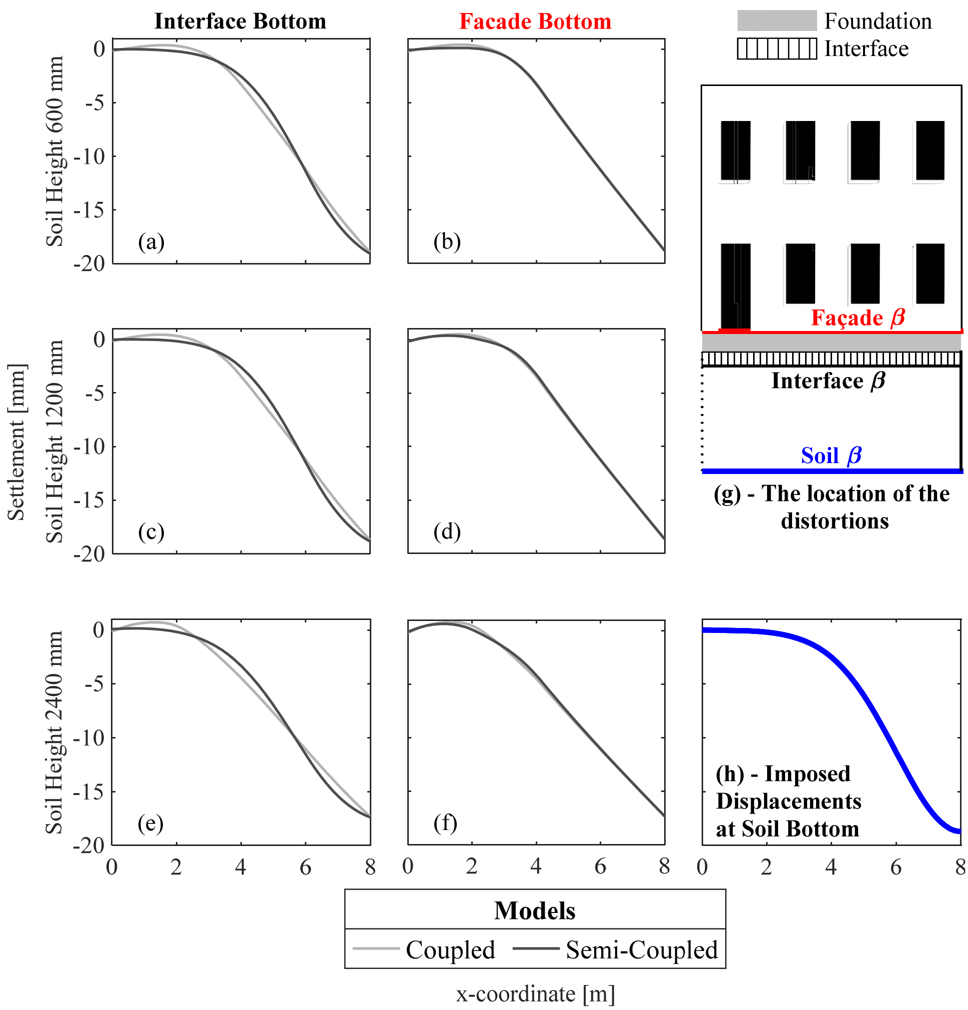

Figure 7 Vertical displacements retrieved for the coupled and uncoupled models in sagging at the last step of the numerical analysis (step 374 with applied angular distortion equal to 1/300) soil height of 600 mm for (a) and (b), 1,200 mm for (c) and (d), 2,400 mm for (e) and (f) (see online version for colours)

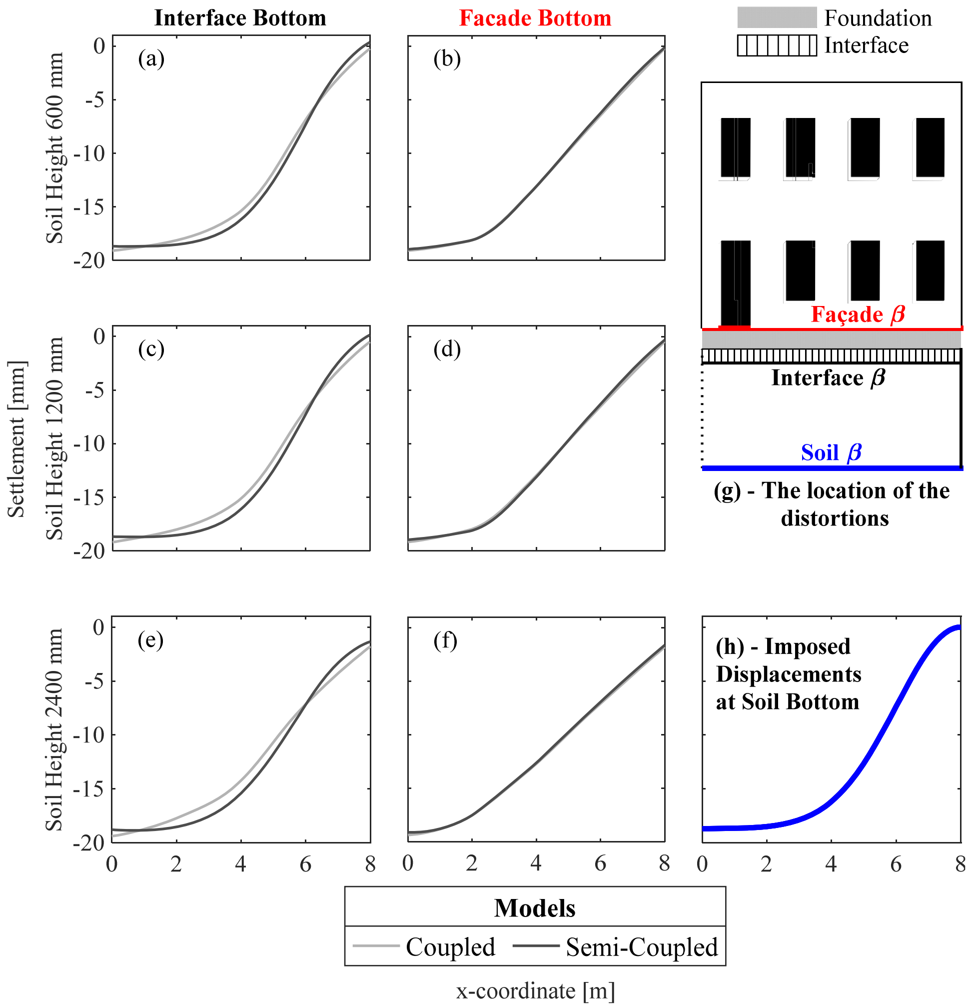

In both the simplified coupled and uncoupled models, the analyses highlight the role of the superstructure and the soil-foundation interface in mitigating the imposed displacements. For both hogging (Figure 6) and sagging (Figure 7) there is no noticeable difference in the displacements observed at the bottom of the façades between the coupled and uncoupled models. This indicates that, despite the different formulations used for contact interfaces in coupled models and boundary interfaces in uncoupled analyses, the superstructure behaves consistently in terms of displacements. However, even if differences may not be immediately noticeable, the displacements measured at the bottom of the façade are not identical between the two modelling approaches for each soil height. Small variations in the displacements measured at the bottom of the façade could still be linked to differences in the distortions and thus the cracking damage between the two models. In fact, according to the definition proposed by Burland and Wroth (1975), the angular distortion refers to the slope of the line connecting two points on the façade relative to the line connecting the two endpoints of the façade. Minor variations in displacement at specific points can lead to noticeable changes in the calculated slope or angle between those points, thereby affecting the overall angular distortion.

Figure 8 Values of the angular distortion at different locations of the models for coupled and uncoupled analyses considering hogging, sagging and different soil heights (see online version for colours)

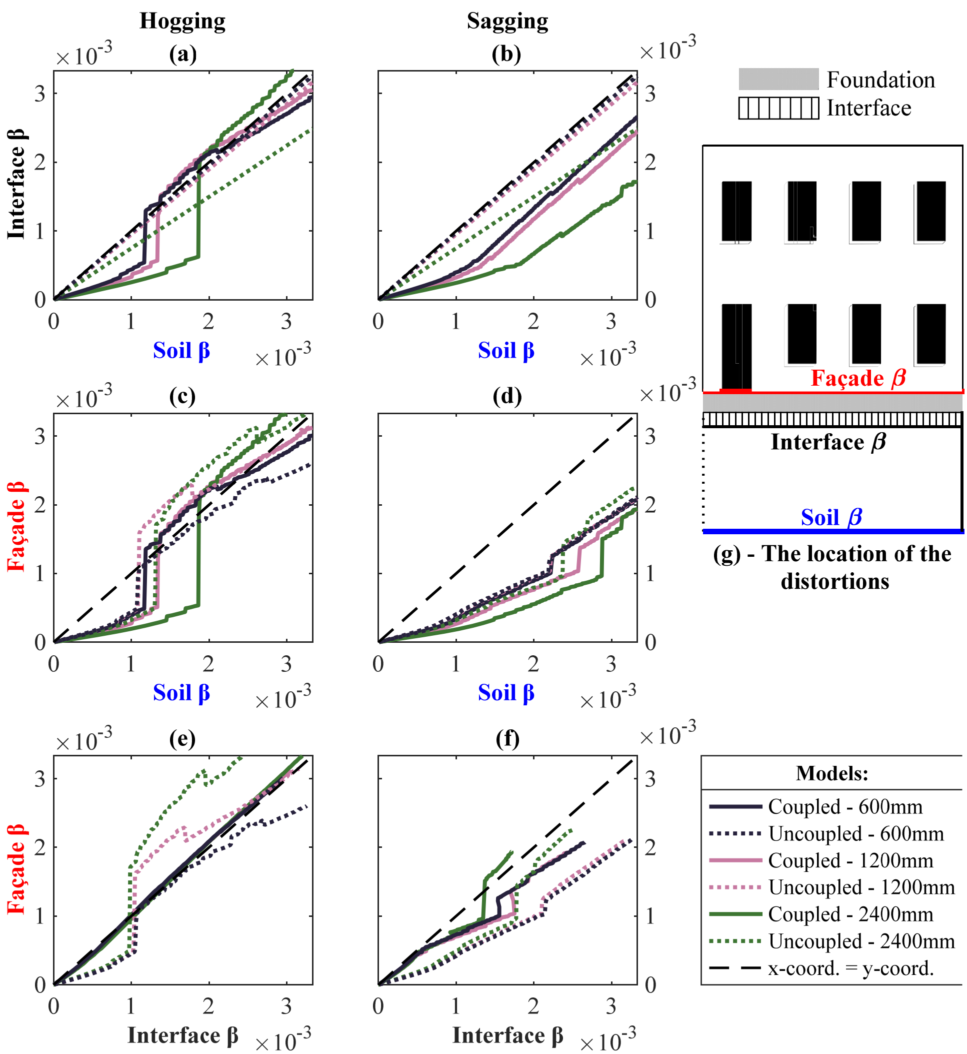

Notes: The values of angular distortion are computed from the displacements at the bottom (soil β) of the soil block and those retrieved at the bottom of the interface (interface β) and the façade (façade β). the black dashed line shows the trend for which the values of the x- and y-axis would be equal. The x-axis ranges between 0 and 1/300.

From the displacements retrieved at the bottom of the soil volume, the interface and the façade [see Figure 6(g) and Figure 7(g)], the values of the angular distortion are computed. Figure 8 shows the relationships between the computed values of the angular distortions from the displacements at the different selected locations. The trends in Figure 8 confirm the observations made in Figure 6 and Figure 7: for coupled models, the distortions applied to the soil experience a significant reduction at the contact interface due to soil-structure interaction [Figures 8(a) and 8(b)]. Then, the distortions transmitted from the interface to the façade are not subject to any further reduction [Figures 8(e) and 8(f)].

In contrast, in uncoupled analyses, the distortions are transmitted from the bottom of the soil to the bottom of the interface with no significant reduction, as this transmission occurs through the linear elastic soil volume [Figures 8(a) and 8(b)]. In uncoupled models, the soil-structure interaction occurs at the interface, which significantly reduces the distortions before they reach the façade [Figures 8(e) and 8(f)].

The comparison of the trends of the applied soil β against the façade β in both sagging and hogging reveals a good agreement of the results of coupled and uncoupled models when the soil height is smaller than 1,200 mm, with the best match observed at 600 mm.

This indicates that, although the displacements at the interface level vary, the types of interfaces used (contact and boundary) do not significantly affect the ratio between the imposed soil deformation and the deformation observed along the façade for small soil heights.

Moreover, in both coupled and uncoupled models, it can be observed that the ratio between the angular distortion values of the soil and the façade [Figures 8(c) and 8(d)] shows a sharp increase, approaching a 1:1 ratio. These increases correspond to damage in the model, either from the formation of new cracks or the sudden widening of pre-existing ones, leading to more flexible behaviour of the façade. As the damage progresses, the façade becomes increasingly flexible, allowing it to better accommodate the imposed settlement deformations. This observation aligns with the conclusions of previous studies (i.e., Prosperi et al., 2023b; Burd et al., 2000).

3.2 *Interface stresses*

The normal interface stresses at the interface have been retrieved for each step of the finite element analyses, for both coupled and uncoupled models. Figure 9 and Figure 10 show the interface stresses of the coupled and uncoupled models with a soil height equal to 600 mm for hogging and sagging respectively at different stages of the numerical analyses. Negligible differences are observed between the interface stresses coupled and uncoupled models during both gravity and the settlement phase. When the gravity load is applied, the entire interface is compressed for both coupled and uncoupled analyses. In the coupled model, the inclusion of soil compression due to gravity results in higher compressive stresses along the transverse walls. The uncoupled model shows compressive stresses localised at the two façade corners. During the settlement application, different locations of the interfaces gradually reach zero compressive stresses, indicating the formation of a gap. The formation of the gap is related to the use of no-tension interfaces, which avoid an unrealistic pulling of the façade due to the ground movements. For instance, a gap is observed to form in the middle of the strip foundation of the façade for sagging [Figures 10(b1) and 10(b2)]. As settlement progresses, the maximum compressive interface stresses become increasingly localised in both hogging and sagging scenarios.

Figure 9 Normal interface stresses (STNy) for hogging for different steps of the analyses for both coupled and uncoupled models with a soil height equal to 600 mm: (a1) and (a2) gravity load; (b1) and (b2) step 112 of the settlement phase (applied soil β equal to 1/1,000); (c1) and (c2) step 374 of the settlement phase (applied soil β equal to 1/300) (see online version for colours)

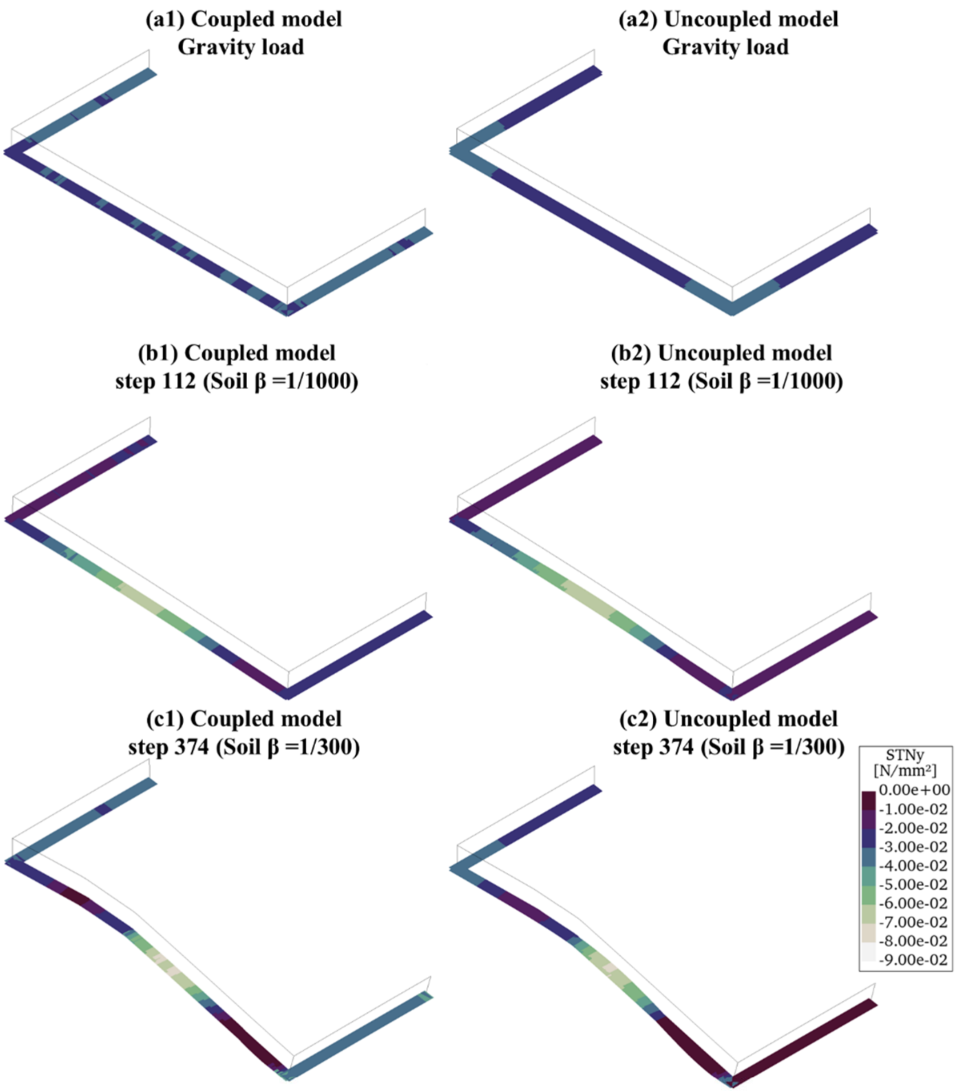

Note: Absolute deformations are shown with a magnification factor equal to 75. Negative values of the normal interface stresses (STNy) represent compression.

3.3 Cracking damage

The values of angular distortion computed from the displacements at the bottom of the soil and the façade are plotted against the computed Ψ values in Figure 11. Overall, the trends confirm the agreement of the results for coupled and uncoupled analyses with a soil height of 600 mm.

Figure 10 Normal interface stresses (STNy) for sagging for different steps of the analyses for both coupled and uncoupled models with a soil height equal to 600 mm: (a1) and (a2) gravity load; (b1) and (b2) step 112 of the settlement phase (applied soil β equal to 1/1,000); (c1) and (c2) step 374 of the settlement phase (applied soil β equal to 1/300) (see online version for colours)

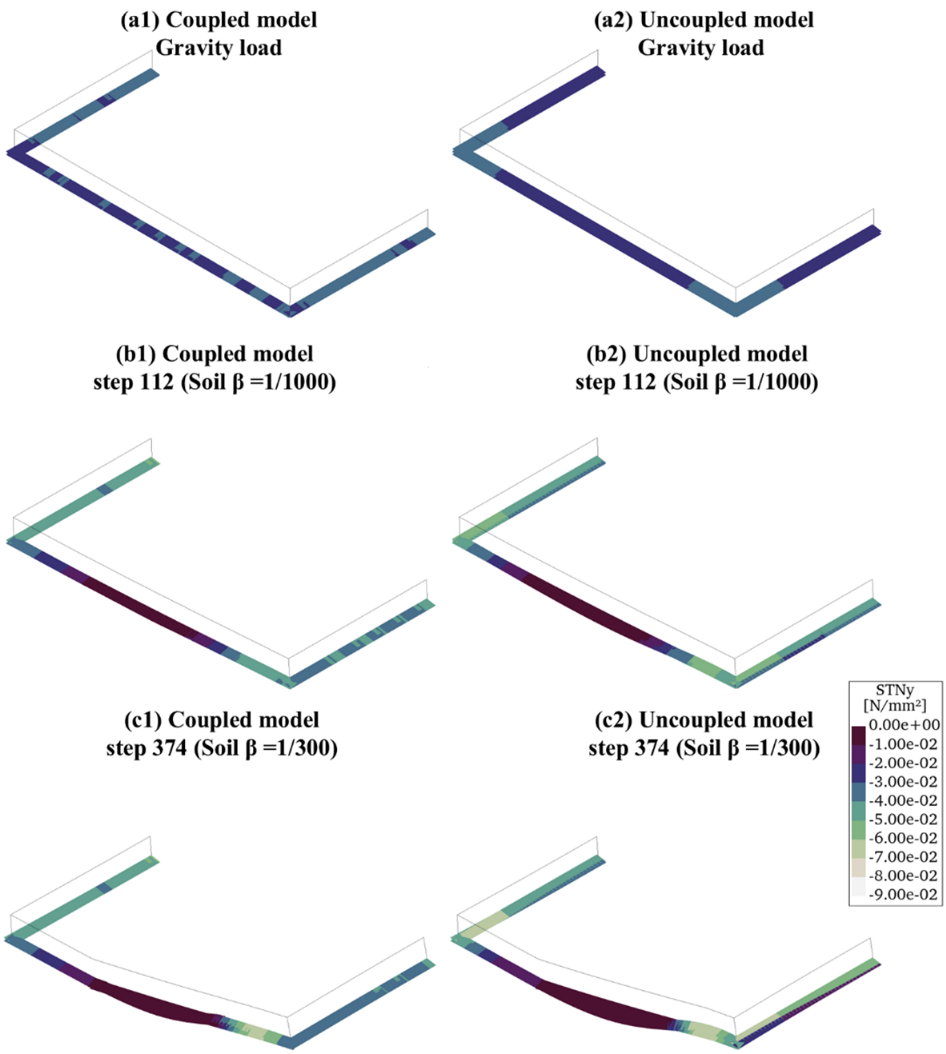

Note: Absolute deformations are shown with a magnification factor equal to 75. Negative values of the normal interface stresses (STNy) represent compression.

As expected, the models with the highest soil height exhibit less damage for the same applied angular distortion at the soil bottom boundary (soil β), as the soil block with a height of 2,400 mm was observed to reduce the imposed distortion.

In general, the uncoupled analyses result in Ψ values slightly higher than the corresponding coupled models for a given soil height and soil β, in both sagging and hogging. The trends also reveal that hogging is a more damaging condition for the structure compared to sagging: for models with a soil height of 600 mm, damage exceeds Ψ equal to 3.0 at a soil β of approximately 1/1,000 in hogging, whereas it occurs at 1/500 in sagging. Therefore, the applied soil β required in sagging for the models with a soil height equal to 600 mm to exceed Ψ equal to 3.0 is 2 times higher than in hogging.

Figure 11 Angular distortion against the resulting damage for all the coupled and uncoupled models for both hogging and sagging (see online version for colours)

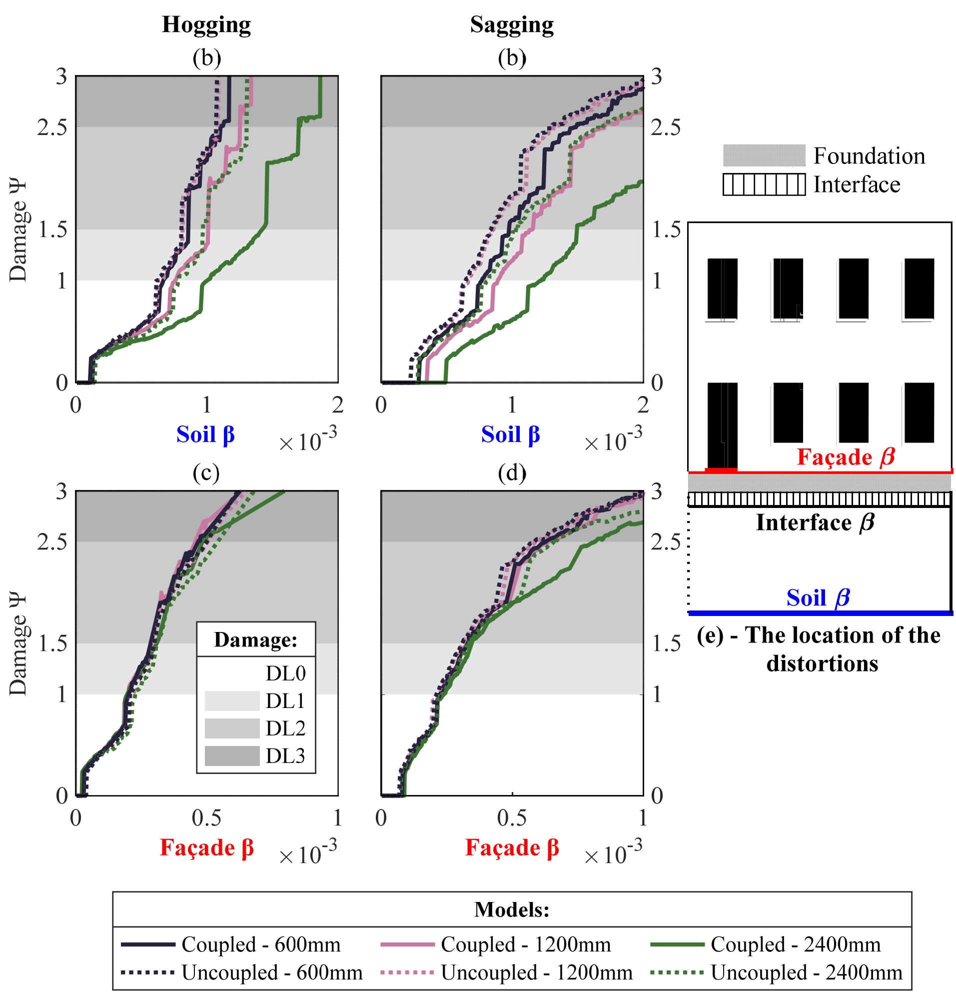

Note: The approximate crack width ranges corresponding to damage parameter Ψ (Table 3) are shown.

Figure 12 Crack patterns in hogging for different steps of the settlement phase for the coupled and uncoupled models with a soil height of 600 millimetres (see online version for colours)

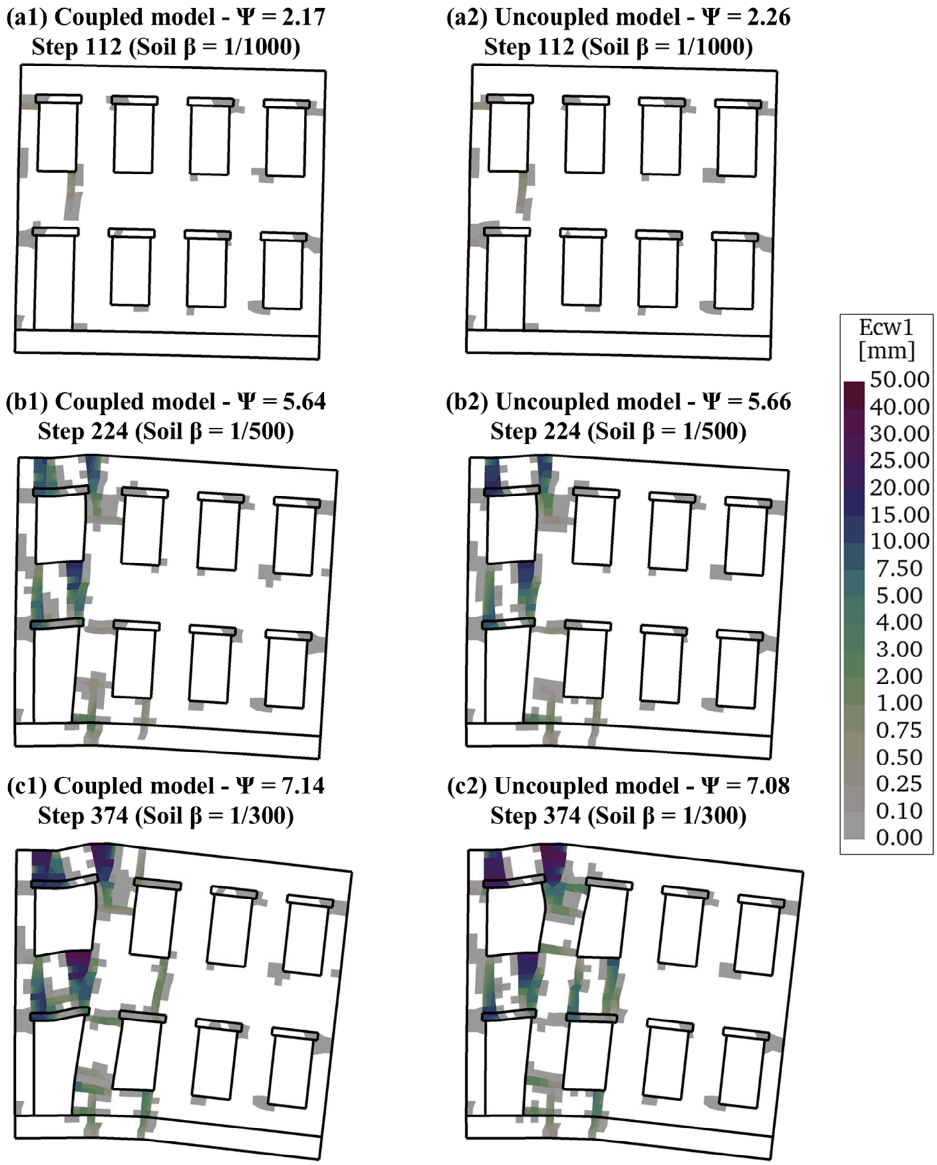

Notes: The contour plots show the maximum crack width in the principal direction (Ecw1). The absolute deformation is shown, with a magnification factor of 30.

Interestingly, the trends in terms of façade β (the angular distortion β computed from the displacements at the base of the façade) and damage Ψ are almost identical across all models in both hogging [Figure 11(c)] and sagging (Figure 11). This confirms that, for a given settlement shape, the façade distortion associated with a certain level of damage is independent of the modelling approach. Conversely, the modelling approach and soil height do influence the amount of applied angular distortion needed to achieve a specific façade distortion, which aligns with the findings of previous studies, such as Prosperi et al. (2023b).

Figure 13 Crack patterns in sagging for different steps of the settlement phase for the coupled and uncoupled models with a soil height of 600 millimetres (see online version for colours)

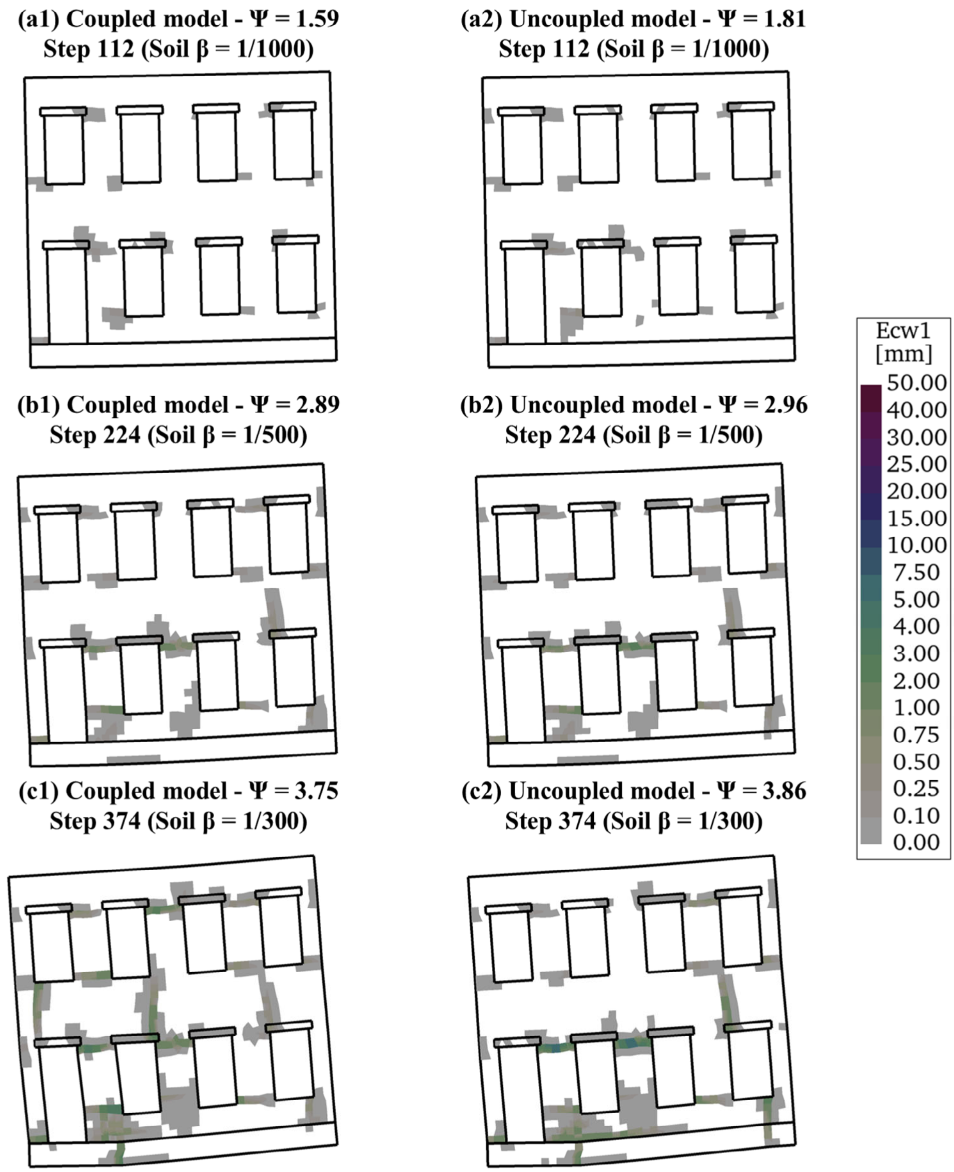

Notes: The contour plots show the maximum crack width in the principal direction (Ecw1). The absolute deformation is shown, with a magnification factor of 30.

Figure 14 Comparison of the crack patterns of the coupled and uncoupled models subjected to hogging for different soil heights at step 112 of the settlement phase (applied soil β equal to 1/1,000) (see online version for colours)

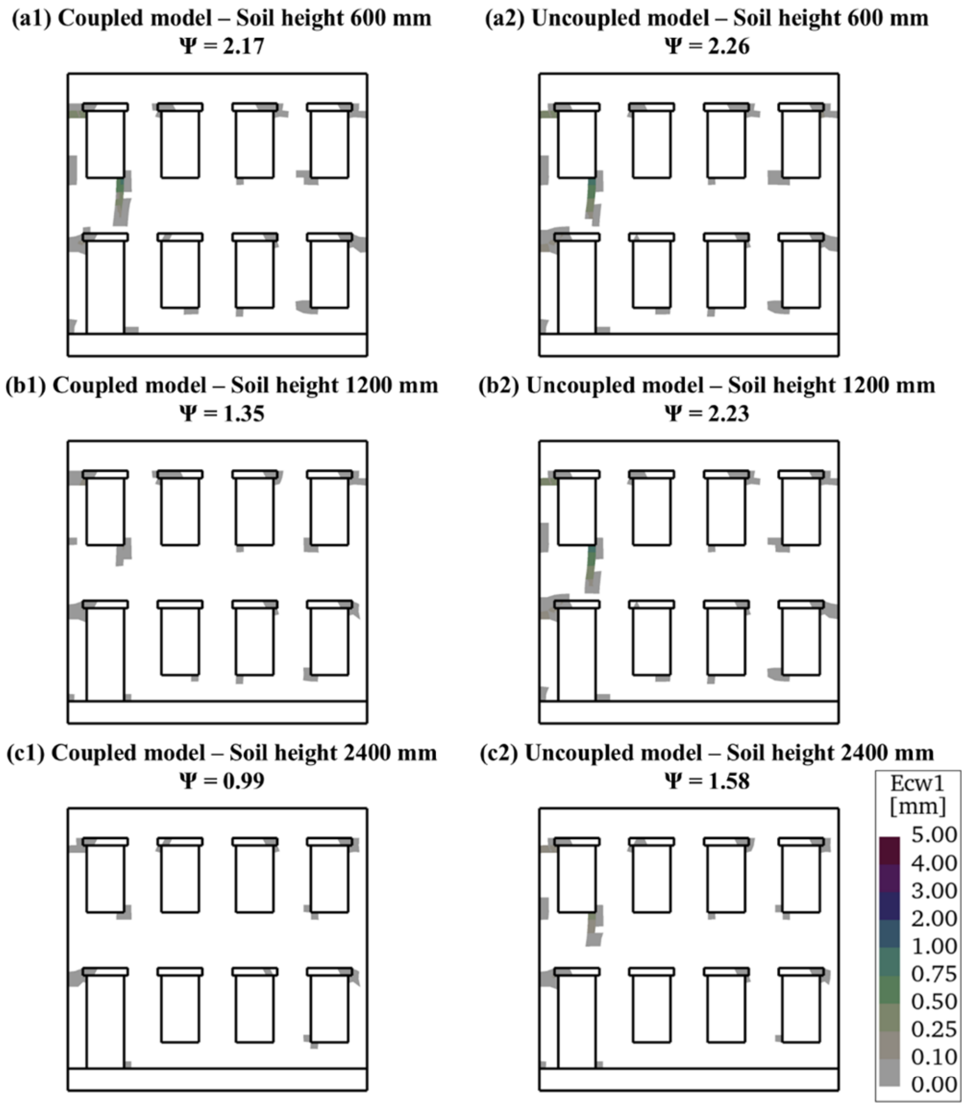

Notes: The contour plots show the maximum crack width in the principal direction (Ecw1). For each model, the value of the damage parameter Ψ is shown. Deformations are not shown.

Further observations can be made by comparing the crack patterns of the models at different stages of the applied settlements. Figure 12 and Figure 13 show the progression of damage for coupled and uncoupled models with a soil height equal to 600 mm in hogging and sagging respectively. For the sake of comparison, the contour plots of the crack patterns are shown for both steps representing light damage and those exceeding it. Both the modelling approaches show similar crack patterns and Ψ values in both hogging and sagging. Cracks initiate at the corners of the openings and propagate mainly vertically and horizontally during the application of the settlements. Interestingly, at the end of the analyses (step 374 in Figure 12 and Figure 13) both the coupled and uncoupled models in hogging and sagging exhibit cracks which develop vertically through the unreinforced masonry strip foundation.

Figure 15 Comparison of the crack patterns of the coupled and uncoupled models subjected to sagging for different soil heights at step 112 of the settlement phase (applied soil β equal to 1/1000) (see online version for colours)

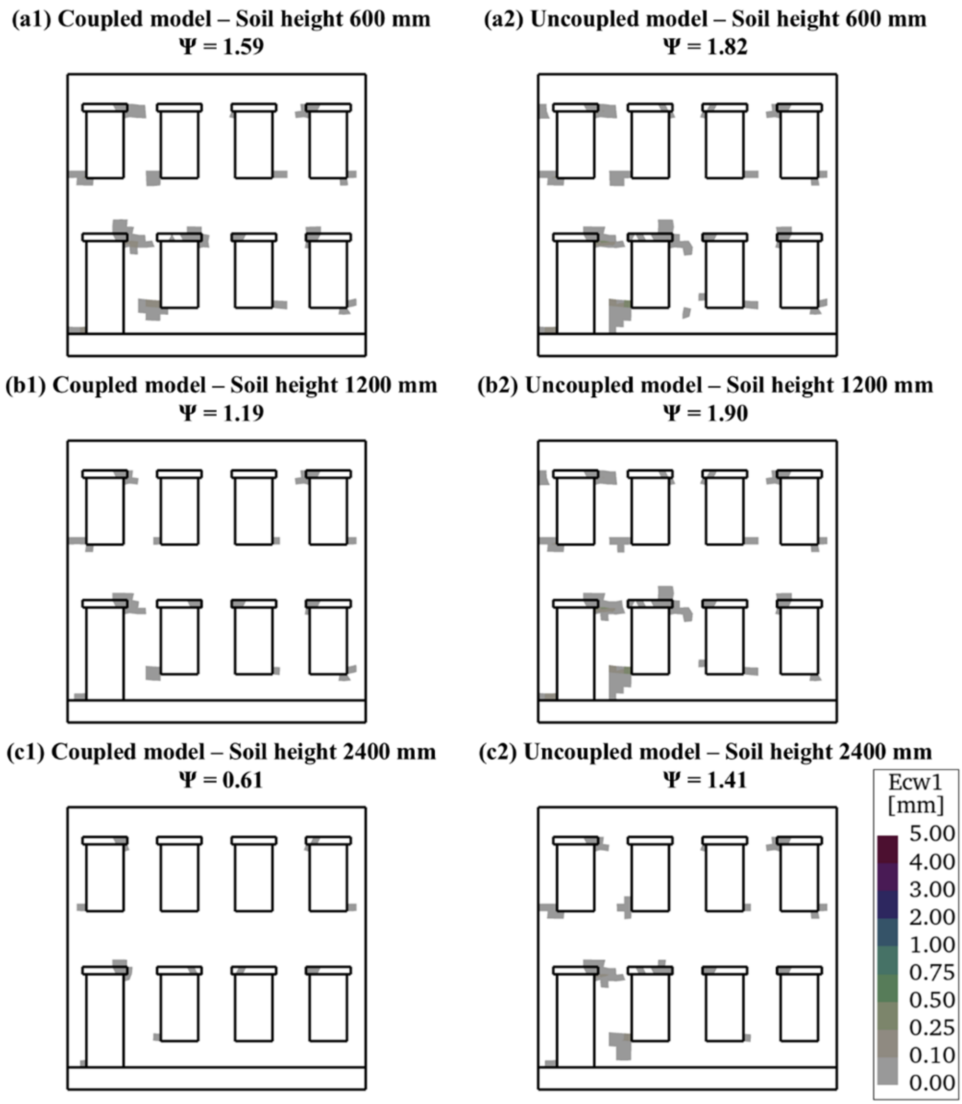

Notes: The contour plots show the maximum crack width in the principal direction (Ecw1). For each model, the value of the damage parameter Ψ is shown. Deformations are not shown.

The influence of the soil height on the crack pattern of the selected models is shown in Figure 14 and Figure 15 for hogging and sagging respectively, for an applied soil β equal to 1/1,000. The results demonstrate that increasing the soil height corresponds to a reduction in damage severity, as the soil volume reduces the imposed distortions in both coupled and uncoupled models. For instance, for models subjected to hogging, when the soil height is increased from 600 mm to 2,400 mm, the damage is reduced by 54% (from 2.17 to 0.99) for coupled models and 30% (from 2.26 to 1.58) for uncoupled models. Similarly, 54.2% (from 1.51 to 0.69) and 22.5% (from 1.82 to 1.41) in sagging for coupled and uncoupled models, respectively.

3.4 Number of elements and nodes

The complexity of two numerical analyses with similar features, i.e., the same element type, nonlinearities, boundary conditions and loadings, can be evaluated by examining the number of elements and nodes. More elements correspond to more nodes, which increase the degrees of freedom, thereby adding complexity to the model and potentially extending the computational time. Table 4 presents the number of elements and nodes for each model. As expected, an increase in soil height leads to an increase in the number of elements and nodes for both coupled and uncoupled models. In general, the number of elements is comparable between the coupled and uncoupled models for each selected soil height. Although the soil volume remains linear elastic, increasing the soil height from 600 to 2,400 mm results in more than doubling the number of nodes.

Table 4 The number of elements and nodes for all the adopted models with a mesh size equal to 200 x 200 mm.

Model		*Soil height [mm]*	*Number of elements*	*Number of nodes*
Coupled		600	4,989	20,845
Coupled		1,200	7,189	29,787
Coupled		2,400	10,489	43,200
Uncoupled	Soil	600	2,200	12,289
	Structure		2,780	8,690
Uncoupled	Soil	1,200	4,400	21,231
	Structure		2,780	8,690
Uncoupled	Soil	2,400	7,700	34,644
	Structure		2,780	8,690

3.5 Analysis time and convergence of each analysis

The performance of all the models can be evaluated in terms of analysis time and number of non-convergent steps. The results are reported in Table 5. The analysis time is normalised by the results of one analysis, arbitrarily selected as reference, i.e., 'coupled model' with a soil height equal to 600 millimetres, for both sagging and hogging settlement.

All the models exhibit similar analysis times, with only minor differences between them. In general, increasing the soil height is associated with longer computational times due to the greater number of elements and nodes. However, this increase is not significant, as the additional nodes are part of the elastic soil volume, which requires less computational effort compared to nonlinear or more complex regions of the model.

Overall, the coupled models tend to have fewer non-convergent steps than their uncoupled counterparts. In coupled models, linking the elastic soil volume directly to the superstructure seems to support numerical stability during the iterative process, resulting in a reduction of non-convergent steps. This effect is more pronounced in sagging than in hogging.

For both coupled and uncoupled analyses, more non-convergent steps are observed in hogging compared to sagging. The cracking damage in hogging progresses and accumulates more quickly than in sagging, as shown in Figure 11 and thus this effect influences the number of non-convergent steps.

Table 5 A comparison of the performance of all the models in both hogging and sagging (see online version for colours)

Model		*Soil height* *[mm]*	*Analysis time* *[hh:mm:ss]*	*Normalised analysis time*	*Number of non-convergent steps*
			Hogging		
Coupled		600	02:22:24	1.00	36
Coupled		1,200	03:15:58	1.38	38
Coupled		2,400	03:05:17	1.30	21
Uncoupled	Soil	600	00:06:13	0.92	0
	Structure		02:05:15		20
Uncoupled	Soil	1,200	00:12:08	1.13	0
	Structure		02:28:09		41
Uncoupled	Soil	2,400	00:20:45	1.10	0
	Structure		02:16:06		49
			Sagging		
Coupled		600	01:38:09	1.00	4
Coupled		1,200	01:48:27	1.10	7
Coupled		2,400	01:48:27	1.10	4
Uncoupled	Soil	600	00:06:12	1.16	0
	Structure		01:47:38		36
Uncoupled	Soil	1,200	00:11:19	1.23	0
	Structure		01:49:40		38
Uncoupled	Soil	2,400	00:19:28	1.15	0
	Structure		01:33:09		21

Note: The values of the coupled models with a soil height of 600 millimetres are shaded.

It is important to note that the analyses presented in this paper focus on the occurrence of ‘light damage’, corresponding to damage parameter (Ψ) values ranging from 0 to 3.0.

Although the settlement is applied to achieve an angular distortion of 1/300, these Ψ values are reached prior to the completion of the settlement phase.

Figure 16 and Figure 17 show non-convergent steps related to the damage progression in each analysis. Notably, non-convergent steps occur when Ψ exceeds 3.0, and therefore, they do not influence the results concerning light damage.

Figure 16 Step number against the number of iterations for each of the selected models subjected to hogging (see online version for colours)

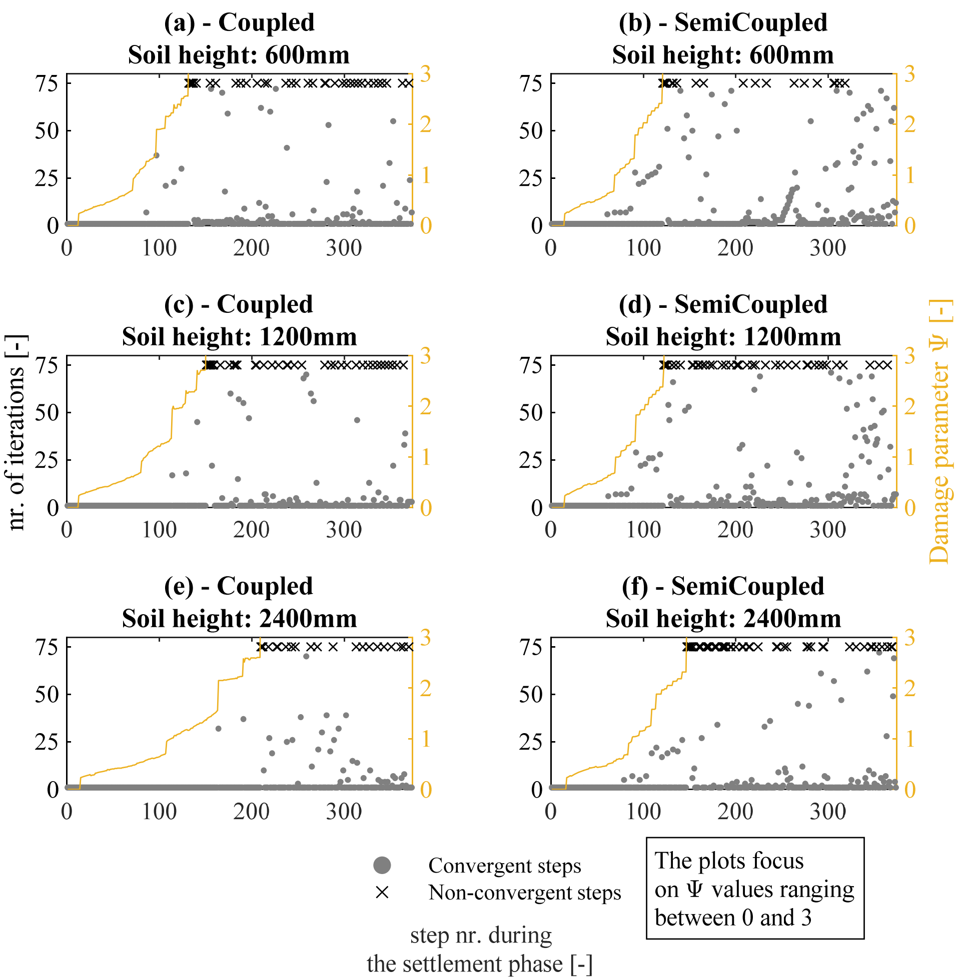

Notes: The plots purposefully focus on Ψ values ranging between 0 and 3.0. The left, y-axis of each plot shows the number of iterations for each step, whereas the y-axis on the damage parameter Ψ. Convergent steps are shown as grey dots, whereas non-convergent steps as black ‘x’ marks.

3.6 *The influence of the mesh size*

Nonlinear finite element analyses of masonry structures can be significantly affected by mesh-dependency issues. The localisation of damage is highly sensitive to mesh size, which in turn can impact the iteration process and the final results of the analysis. To evaluate this effect, different mesh sizes, such as 100 × 100 mm and 50 × 50 mm (see Figure 18) were used for both coupled and uncoupled models with a soil height of 600 mm. These results are compared with those obtained from models previously using a 200 × 200 mm mesh size. The results of the sensitivity analyses are shown in Figure 19.

Figure 17 Step number against the number of iterations for each of the selected models subjected to sagging

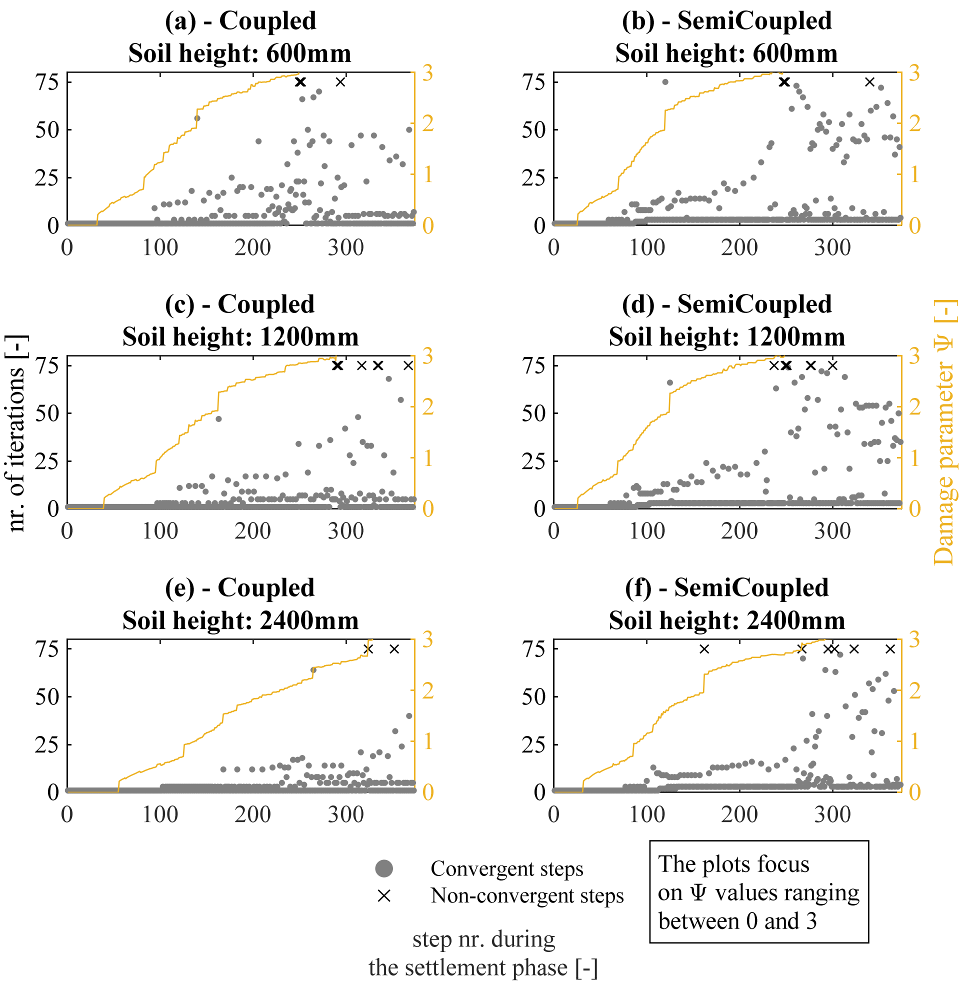

Notes: The plots purposefully focus on Ψ values ranging between 0 and 3.0. The left, y-axis of each plot shows the number of iterations for each step, whereas the y-axis on the damage parameter Ψ. Convergent steps are shown as grey dots, whereas non-convergent steps as black 'x' marks.

The trends of the applied soil β with respect to the damage parameters Ψ are similar for both sagging and hogging in both coupled and uncoupled analyses (Figure 19). In particular, for sagging, only minor differences are observed (Figure 19c and d), whereas more significant differences are noted for hogging (Figure 19a and b). Specifically, for hogging the trends of the applied soil β with respect to the damage parameters Ψ show differences for values of Ψ higher than 1.5.

Figure 18 The different mesh sizes selected for the sensitivity analysis, (a) mesh size 200 × 200 mm (b) mesh size 100 × 100 mm (c) mesh size 50 × 50 mm

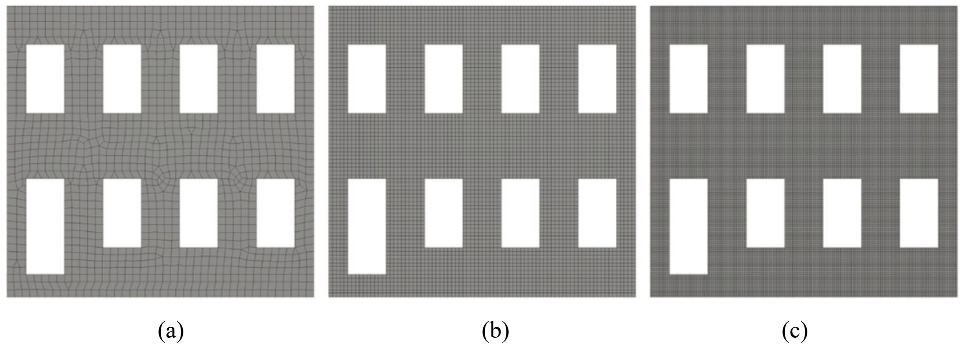

Figure 19 Results of the numerical models in terms of imposed angular distortion against the resulting damage for selected mesh sizes in both hogging and sagging (see online version for colours)

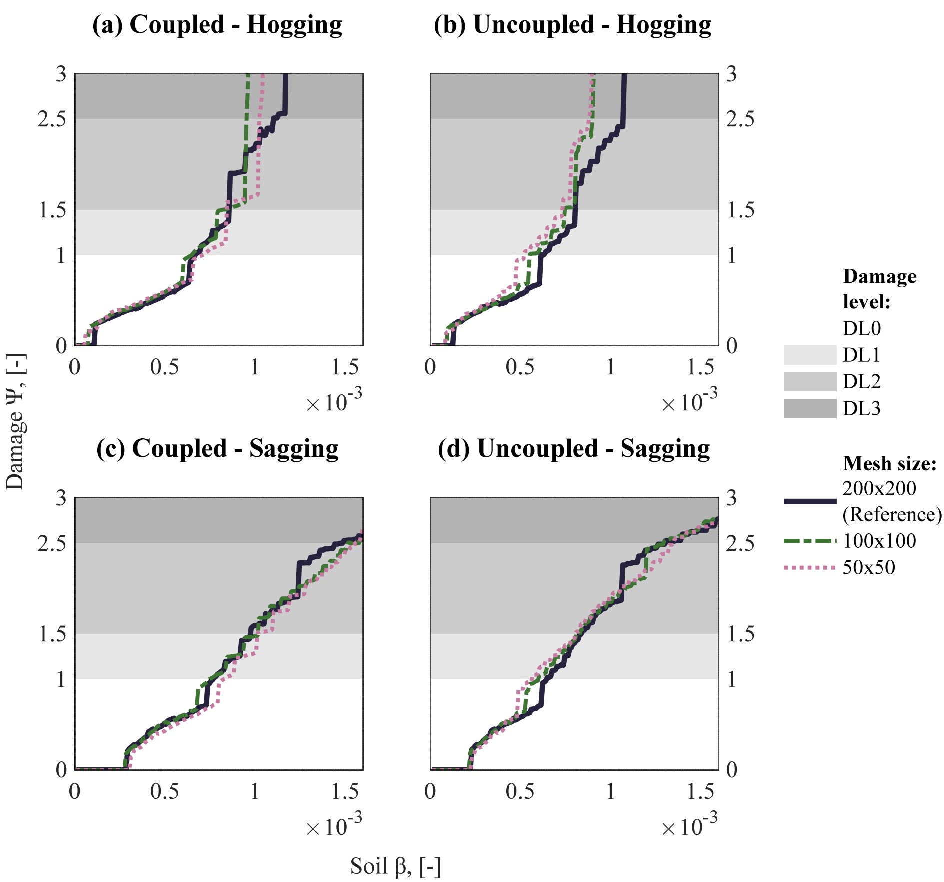

The differences can be attributed to variations in the iterative solution process and model convergence, which result from the different mesh sizes. Figure 20 shows the number of non-convergent steps for each model, with a focus on hogging. A few non-convergent steps occur even before Ψ exceeds 3.0 for the 100 x 100 mm and 50 x 50 mm mesh sizes, which helps explain the differences in the trends shown in Figure 19.

Figure 20 Step number against the number of iterations for each of the coupled and uncoupled models subjected to hogging with a soil height equal to 600 mm and for different mesh sizes (see online version for colours)

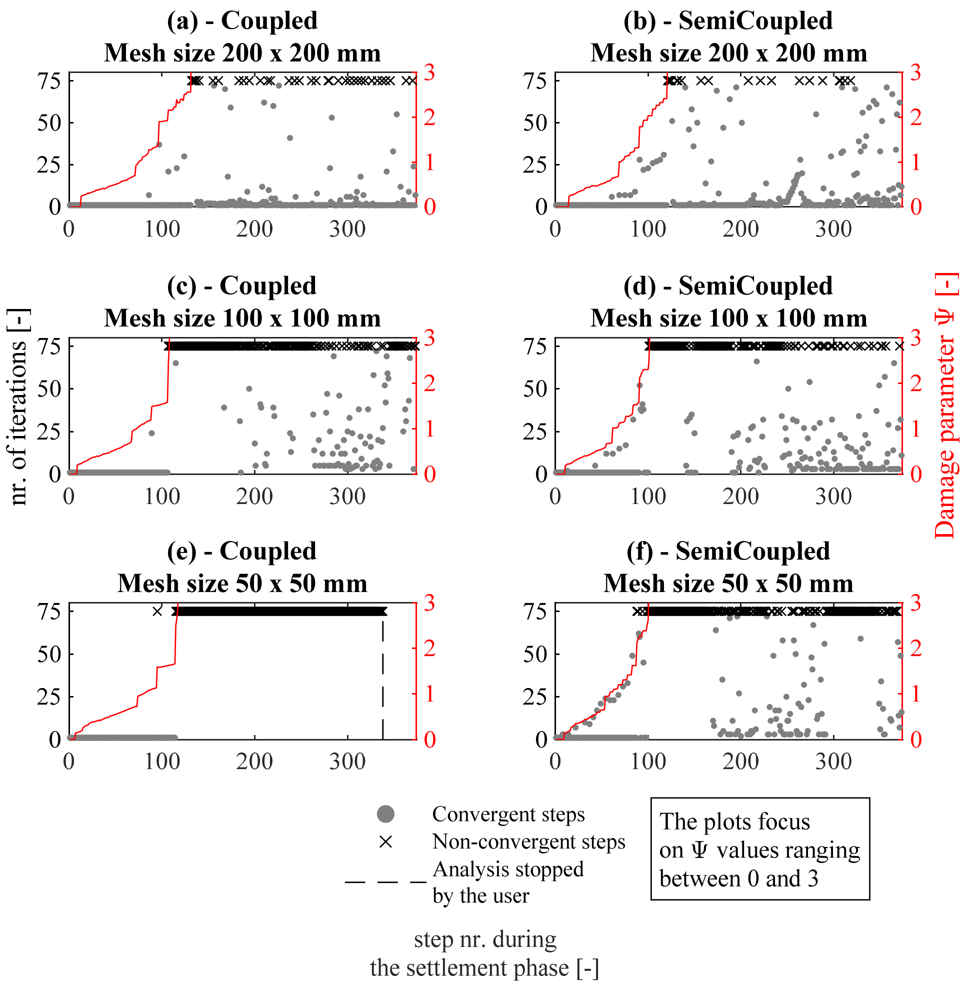

Notes: The plots purposefully focus on Ψ values ranging between 0 and 3.0. The left, y-axis of each plot shows the number of iterations for each step, whereas the y-axis on the damage parameter Ψ. Convergent steps are shown as grey dots, whereas non-convergent steps as black 'x' marks.

It can be observed that the number of non-convergent steps occurring after the damage exceeds Ψ values higher than 3.0 increases as the mesh size decreases, for both coupled and uncoupled models. In particular, for the coupled model with a mesh size of

50 × 50 mm, the analysis was stopped by the user because convergence was never achieved once the damage exceeded light damage levels. In contrast, for the other analyses, both convergent and non-convergent steps are observed once the damage exceeds light damage levels.

Decreasing the mesh size is associated with an increase in the required computational time: for example, the analysis of the uncoupled model with a mesh size of 50 × 50 mm, when subjected to hogging, took approximately 100 times longer (i.e., 7–8 days) compared to the same model with a 200 × 200 mm mesh size. This effect is attributed not only to the increased number of elements and nodes but also to a greater number of non-convergent steps caused by the smaller mesh size.

Figure 21 Comparison of the crack patterns of the coupled model with a soil height of 600 mm in hogging for the different selected mesh sizes at different angular distortion

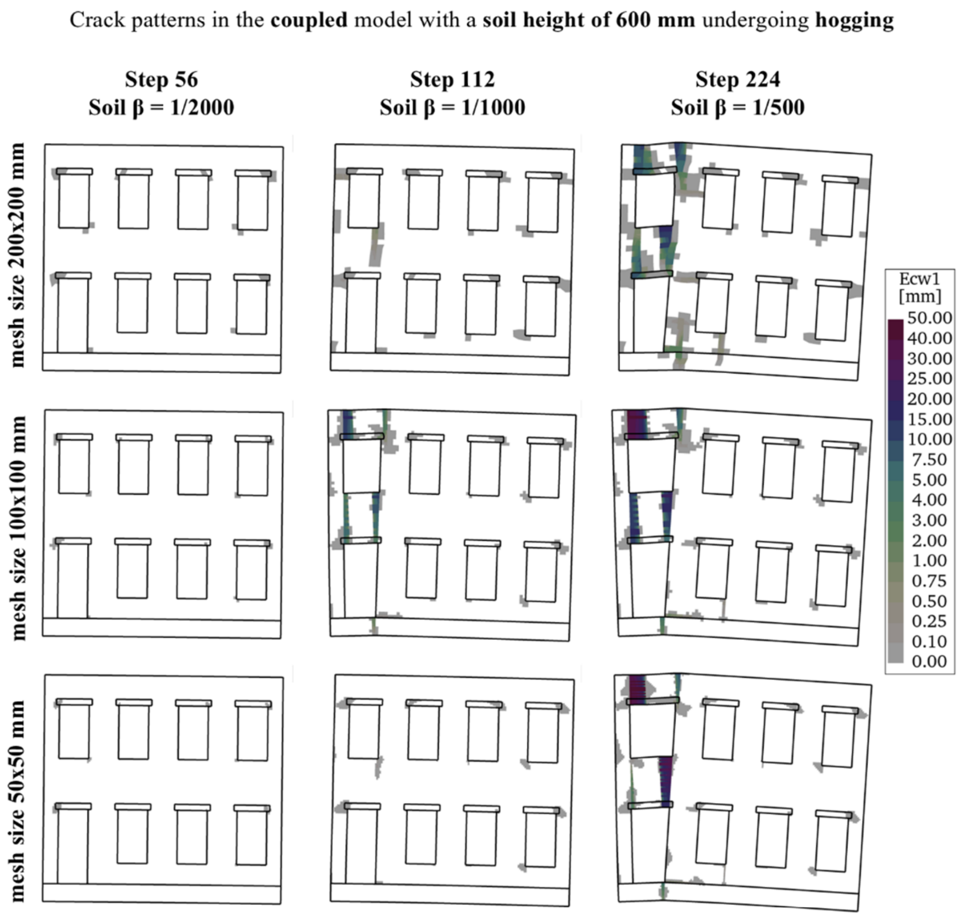

Notes: The contour plots show the maximum crack width in the principal direction (Ecw1).
The absolute deformation is shown with a magnification factor equal to 30.

To further assess the impact of the mesh on the numerical results, Figure 21 presents the crack patterns at various stages of hogging settlements for the coupled model with a soil height of 600 mm: The first two selected steps, '56' and '112,' provide insights into the results of the models that do not exceed light damage (Ψ less than 3.0). In contrast, in the last step, '224', the models have already exceeded light damage, during which non-convergent steps become prevalent in the analyses. For an applied angular distortion equal to 1/2,000, all the crack patterns show consistent results. When the applied angular distortion is increased to 1/1,000, the crack patterns for the models with mesh sizes of 200 × 200 mm and 50 × 50 mm are consistent, while more severe damage is observed in the model with a 100 × 100 mm mesh size. It appears that cracks in the 100 × 100 mm mesh models open suddenly, leading to a sharp increase in damage, as confirmed by the trends shown in Figure 19. However, when the applied angular distortion is set to 1/500, all analyses again exhibit a consistent crack pattern. Therefore, variations in mesh size are linked to changes in the values of applied angular distortion required to achieve a specific level of damage severity. These changes are influenced by both the localisation of cracks, which varies with mesh size, and the increased number of non-convergent steps observed with smaller mesh sizes.

4 Discussion

This study carried out a comparison between two different 3D modelling approaches to evaluate the response of masonry structures on strip foundations exposed to subsidence. The analyses considered a simplified coupled approach, in which the soil and the superstructure are modelled together, and an uncoupled approach, in which the soil and the structure are separated in two different models. The structural subsystem of the uncoupled (semi-coupled) approach has been used in previous studies to simulate the response of buildings affected by settlements (e.g., Prosperi et al., 2023b; Longo et al., 2021). In this work, the simplified coupled approach is proposed as an alternative modelling technique to compare the outcomes of both models.

In both the selected modelling approaches, the height of the linear-elastic soil volume represents the shallow soil layers supporting the foundation, while deeper layers, where subsidence may occur, are not modelled.

Unlike earlier studies that primarily emphasise settlement due to tunnel excavation, mining, or similar activities, subsidence can also result from other factors, such as groundwater depletion, peat oxidation, clay shrinkage, or a combination of multiple drivers. This underscores the importance of employing detailed soil models that incorporate these settlement drivers to accurately simulate soil-structure interaction and the associated settlements. Such an approach is essential for both fully-coupled and uncoupled models (Giardina et al., 2013a; Burd et al., 2000, 2022; Ninić et al., 2024; Bilotta, 2017). However, prior research often focuses on the effect of a single cause of settlement. In this study, the emphasis is placed on settlement arising from subsidence processes. The modelled settlement patterns reflect asymmetric hogging and sagging deformations caused by subsidence in deeper soil layers not explicitly represented in the models. A key advantage of this modelling method is that it applies settlement displacements at the lower boundary of the soil volume, effectively idealising subsidence while simplifying the model. Nevertheless, the chosen coupled approach does not account for the interaction between the building, the soil, and the settlement drivers, leading to its designation as a 'simplified coupled' model. Incorporating the linear-elastic soil volume into the simplified coupled model has been thus proposed as a technique to aid the representation of soil-structure interaction with the superficial soil layer. The soil is tied to the superstructure employing 'contact' interface elements, and their normal and tangential stiffness is computed from the properties of the adjacent soil. In the uncoupled model, settlement displacements are initially applied to the linear-elastic soil subsystem. Although the soil is modelled as a linear-elastic continuum, a minor reduction in the distortion of the applied displacement fields may occur. Therefore, the soil subsystem is included to ensure a consistent comparison with the simplified coupled model. The displacements retrieved at the top of the soil volume are then applied to the structural subsystem. In particular, the retrieved displacements are subsequently applied at the bottom of the 'boundary' interface elements at the base of the façade foundation.

Regarding the differences in the analytical formulations used to estimate normal and tangential stiffnesses for contact and boundary interfaces, the formulations for contact interfaces require two soil parameters and the mesh size of the numerical model. In contrast, the formulations for boundary interfaces depend on two soil parameters as well as two additional geometric parameters: the foundation length and the foundation base. The vertical stiffness computed for boundary interfaces in uncoupled models is approximately five times lower than those used for contact interfaces. This lower value is consistent with the fact that boundary interfaces also account for the behaviour of the soil volume that is absent from the structural subsystem in the uncoupled model.

The applied settlement shapes localise the distortion along the façade of the buildings, whereas there are no variations perpendicular to the plane of the façade. Moreover, this study focuses on vertical displacements purposively neglecting the horizontal components. While for excavations, tunnelling or mining works horizontal displacements have a great influence on the behaviour of the structures, their magnitude is significantly smaller for other sources of settlements, which represents the focus of this study (Prosperi et al., 2023b; Boscardin and Cording, 1989). Thus, the horizontal ground deformations are herein purposively neglected.

This study focuses on the cracking damage which initiates and propagates on the façade, as settlement shapes do not present three-dimensional variations along transversal walls. Therefore, the models are characterised by structural symmetry and therefore, only half of the model is depicted, including the façade and a half portion of each transverse wall.

The adopted constitutive model for the masonry material, the EMM, offers strong numerical stability and reliable convergence (Sousamli, 2024) and has been observed to accurately replicate crack patterns from experiments with satisfactory accuracy (Korswagen, 2024). Nevertheless, the model has limitations in damage localisation, with cracks appearing as diffuse rather than sharply localised (Schreppers et al., 2016; Sousamli, 2024). The analyses, herein presented, focus on the occurrence of 'light' damage due to settlements, associated with cracks not wider than 5 mm (and a damage parameter Ψ of 3.0 to 3.5 or less). For more severe damage, cracking may not be the most reliable indicator, as such damage could compromise the structural capacity and potentially lead to collapse.

The results of the two selected modelling approaches are compared in terms of displacements, stresses at the interface and cracking damage. The influence of soil volume is also examined by varying the soil height parameter, which represents the depth of the linear-elastic soil layer included in the models. It has been observed that, for both modelling approaches, increasing the soil volume reduces the magnitude of the distortions transmitted to the façade, thereby flattening the imposed deformation. In other words, the ratio between the distortions applied at the bottom of the soil and the ones retrieved at the bottom of the façade is influenced by the soil height. This reduction is also affected by structural damage and the shape of the imposed settlement, as increased damage can make the façade more flexible and cause it to more closely follow the imposed settlements. For example, in models subjected to hogging settlements with the smallest soil height (600 mm) and an applied distortion (soil β) of 1/2,000, the resulting distortion at the bottom of the façade (façade β) is approximately 1/6,000, making it three times smaller. Conversely, when the soil β is 1/1,000, the façade β is approximately 1/2000, which is two times smaller.

For each settlement shape, the crack pattern, i.e., the amount, location and orientation of cracks, is consistent between coupled and uncoupled models. However, the damage severity is influenced by the soil volume. For a given applied distortion, models with greater soil height exhibit less damage. For example, with an applied angular distortion of 1.0‰ (or 1/1000), the coupled model in hogging shows Ψ values of 2.2, 1.4, and 1.0 for soil heights of 600 mm, 1,200 mm, and 2,400 mm, respectively. The most conservative predictions, indicating higher damage, are observed in models with the smallest soil height, both in sagging and hogging, for both modelling approaches. Moreover, the differences in the damage severity, quantified by Ψ, between coupled and uncoupled analyses for each soil height can be attributed to the differences in the distortions measured on the facades in each step of the analyses. As previously discussed, while the differences in displacements observed on the façade may not be immediately noticeable, angular distortion is sensitive to even small variations. This sensitivity helps explain the discrepancies between the models. Overall, the uncoupled models show slightly higher damage than their coupled counterparts. This observation is consistent with the conclusions in Burd et al. (2000).

The relationship between the distortion measured on the façade and the damage depends on the shape of the settlement and is not influenced by the modelling approach. Minor discrepancies are observed only for the largest soil height of 2,400 mm. This difference can be attributed to the fact that increasing the soil height can affect both the magnitude of the distortions and the shape of the settlement experienced by the façade.

Moreover, for a given applied distortion, the damage on the façade is observed to be more severe in hogging than in sagging for both modelling approaches; this is consistent with the state-of-the-art (Giardina et al., 2013a; Burd et al., 2000; CEN, 2004). For instance, for an applied distortion equal to 1/1,000, the coupled model with the smallest soil volume shows a Ψ equal to 2.2 in hogging, whereas Ψ equals 1.6 in sagging, thus 1.4 times smaller.

The contribution of the soil subsystem in the uncoupled models was found to be negligible for a soil height of 600 mm. This supports the notion that the settlement pattern can be directly applied to the superstructure subsystem, aligning with the methodology used in previous studies, such as Korswagen et al. (2023).

Interestingly, despite that the analytical formulation used for boundary interfaces in uncoupled models considers the soil as a homogeneous half-space, the closest agreement with the coupled models is observed for a soil height of 600 mm. This observation can be attributed to the fact that the coupled models offer an alternative modelling approach rather than serving as a calibration or validation model for the uncoupled models. Additional calibration and validation using a case study with detailed information could further clarify the influence of the soil volume. A more comprehensive model could be developed by incorporating deeper soil layers, accounting for their nonlinearity, and considering the impact of various triggers for subsidence processes. For an objective comparison, ‘green-field’ settlements, resulting solely from the soil volume, including deeper layers, nonlinear soil behaviour, and subsidence drivers without the influence of structures, can be applied to the structural subsystem of the uncoupled model. These results should then be compared with those from a fully coupled model incorporating the same soil volume. However, modelling specific subsidence drivers such as groundwater lowering, organic matter oxidation, and seasonal groundwater fluctuations adds significant complexity, as previously mentioned. Consequently, this study intentionally omits the nonlinear behaviour of the soil and the inclusion of such subsidence drivers.

It remains uncertain whether the selected modelling strategies can accurately predict the response of existing structures. However, it is important to note that similar modelling strategies have been successfully used in previous studies to replicate the behaviour of existing structures or experimental benchmarks with good agreement, as seen in Drougkas et al. (2020), Giardina et al. (2013b) and Bejarano-Urrego et al. (2019).

Both modelling approaches show comparable complexity in terms of the number of elements and nodes, as well as performance regarding computational time and convergence. However, these factors do not address the time, the modelling burden or the expertise and knowledge required to build the models since these aspects can be highly subjective.

Although numerical analyses that account for cracking and post-cracking softening behaviour in masonry are affected by mesh-dependent behaviour (Yiu et al., 2017), the mesh size has been found to have no significant impact on the overall damage mechanism of the considered models. The crack pattern is consistent throughout the application of the settlements, as cracks initiate and progress in the same locations. However, the mesh size influences at which step of the analysis some cracks open, and, in turn, the relationship between the distortion and damage is thus affected. Further analyses could explore how variations in the settings of the numerical analyses impact the model outcomes. For instance, adjusting the iterative method used for numerical solutions, or changing the type of convergence norm and its tolerance, could provide additional insights.

When choosing between the adopted modelling strategies, a fully- or simplified-coupled model may be more suitable for scenarios involving multiple overlapping simultaneous effects. For example, it can effectively manage both vertical displacements at the base of the soil volume, assessed through angular distortion, and horizontal displacements, measured by horizontal strains applied to the sides of the soil volume. On the other hand, an uncoupled model might be preferable for evaluating structures exposed only to vertical displacements. In such cases, the minimal influence of the soil stratum allows for a direct application of settlement shapes to the superstructure, simplifying the evaluation process and reducing modelling complexity.

5 Conclusions

This study proposed a mutual comparison between two different 3D modelling approaches to evaluate the response of masonry buildings on shallow foundations undergoing subsidence: a coupled model, in which the soil is tied to the superstructure, and an uncoupled model, in which the soil is modelled separately from the structure. Displacements are applied to the bottom of the soil volume in both modelling approaches, and the deformations are consequently transmitted from the soil to the superstructure using interface elements. The analyses focus on light damage comprising small masonry cracks. The aim is to evaluate the performance of the selected models and investigate their differences. Thus, it was observed that:

- The height of the soil volume, included in both simplified coupled and uncoupled models, significantly impacts the displacements transmitted to the structure. Increasing the soil volume height reduces the distortions transmitted to the superstructure and, in turn, the damage severity associated with the imposed distortions. Additionally, a higher soil height amplifies the differences in displacements, and stresses, between the coupled and uncoupled models, and leads to a higher computational time.
- Angular distortion is used to quantify the intensity of both the distortion applied at the bottom of the models and the distortions observed throughout the building. This parameter is highly sensitive to even small changes in displacements, as it measures the relative slope between points on a structure. As a result, angular distortion allows for detecting even small differences in displacements between coupled and uncoupled models, which can be effectively linked to the extent of damage.
- Different displacements are observed beneath the interface in the coupled and uncoupled models. In coupled models, the imposed distortion is significantly reduced at the interface level, but only slightly decreases at the façade level. In contrast, for uncoupled models, the distortion at the top of the soil volume remains largely unaffected by the soil stratum and is equal to the imposed distortion at the bottom. However, it flattens out as it reaches the bottom of the façade.
- The relationship between the distortions calculated from the façade displacements and the resulting damage is not affected by the soil height. While the height of the soil volume does influence the ratio between the applied distortions and those transmitted to the façade, a specific damage intensity will consistently be observed once the distortion experienced by the façade reaches a certain threshold, which depends instead on the shape of the settlements.
- The coupled and uncoupled models have been observed to produce consistent results in terms of damage, displacements and stresses for a soil height equal to 600 millimetres.
- The crack patterns, i.e., the location and orientation of the cracks, developed during the application of the settlements, are observed to be consistent between the two modelling approaches, regardless of soil height.
- After damage initiates, uncoupled models exhibit slightly more damage than coupled models for a given level of imposed angular distortion, up to the point where light damage is exceeded. Consequently, they are considered to be more conservative.
- Both the coupled and uncoupled models contain a similar number of elements and nodes, resulting in comparable performance in terms of computational time, convergence, and mesh dependency, regardless of the soil height. Overall, coupled analyses seem to achieve slightly better convergence. However, non-convergent steps are observed in the numerical analyses only once light damage has been exceeded.

- Reducing the mesh size increases computational time and the number of non-convergent steps in the numerical analyses. Consequently, while the overall damage mechanism of the façade remains consistent, the localisation and progression of cracks are impacted. This leads to variations in damage severity at different steps. Therefore, the imposed distortions required for the model to exhibit a specific level of damage are influenced by the mesh size, as cracks may progress more rapidly at different stages of the analysis.
- In both modelling approaches, damage to the façade is determined by its deformation, which is directly influenced by the shape of the imposed settlements.
- The coupled models presented herein offer an alternative strategy for modelling soil-structure interaction compared to uncoupled models. While both the coupled and uncoupled models produce similar results and performance, the uncoupled model may be better suited for evaluating the response of structures subjected solely to vertical displacements. In the case of uncoupled models with small soil heights, the limited contribution of the soil stratum allows the superstructure subsystem to be used directly, simplifying the evaluation of structures under vertical displacements and reducing the modelling complexity.

Declarations

The research presented in this paper is part of the project Living on Soft Soils: Subsidence and Society (grantnr.: NWA.1160.18.259). This project is funded by the Dutch Research Council (NWO-NWA-ORC), Utrecht University, Wageningen University, Delft University of Technology, Ministry of Infrastructure & Water Management, Ministry of the Interior & Kingdom Relations, Deltares, Wageningen Environmental Research, TNO-Geological Survey of The Netherlands, STOWA, Water Authority: Hoogheemraadschap de Stichtse Rijnlanden, Water Authority: Drents Overijsselse Delta, Province of Utrecht, Province of Zuid-Holland, Municipality of Gouda, Platform Soft Soil, Sweco, Tauw BV, NAM.

References

Bejarano-Urrego, L., Verstrynge, E., Drougkas, A., Giardina, G., Bassier, M., Vergauwen, M. and Van Balen, K. (2019) 'Numerical analysis of settlement-induced damage to a masonry church nave wall', in *Structural Analysis of Historical Constructions: An Interdisciplinary Approach*, pp.853–861, Springer International Publishing.

Bilotta, E. (2017) 'Soil-structure interaction in tunnel construction in soft ground', *Rivista Italiana di Geotechnica*., Vol. 51, No. 2, pp.5–30.

Bilotta, E., Paolillo, A., Russo, G. and Aversa, S. (2017) 'Displacements induced by tunnelling under a historical building', *Tunn. Undergr. Sp. Tech*., January, Vol. 61, pp.221–232.

Boscardin, M.D. and Cording, E.J. (1989) 'Building response to excavation-induced settlement', *J. Geotech. Eng-Asce*., Vol. 115, No. 1, pp.1–21.

Bowles, J. (1988) *Foundation Analysis and Design*, 1 February, McGraw-Hill, Inc., USA.

Burd, H., Houlsby, G., Augarde, C. and Liu, G. (2000) 'Modelling tunnelling-induced settlement of masonry buildings', *PI Civil Eng-Geotec*., Vol. 143, No. 1, pp.17-29.

Burd, H., Yiu, W., Acikgoz, S. and Martin, C. (2022) 'Soil-foundation interaction model for the assessment of tunnelling-induced damage to masonry buildings', *Tunn. Undergr. Sp. Tech.*, Vol. 119, No. 2022, p.104208.

Burland, J.B. and Wroth, C. (1975) 'Settlement of buildings and associated damage', No. CP 33/75.

Burland, J.B., Broms, B.B. and De Mello, V.F. (1979) 'Behaviour of foundations and structures', pp.495–546.

CEN (2004) *Eurocode 7 Geotechnical design – Part 1: General Rules*, Final Draft, EN 1997-1:2004 (E), (F) and (G). European Committee for Standardization, Brussels, p.168 pages (E).

Charles, J.A. and Skinner, H.D. (2004) 'Settlement and tilt of low-rise buildings', *P I Civil Eng-Geotec*., Vol. 157, No. 2004, pp.65–75.

Dalgic, K.D., Gulen, B., Liu, Y., Acikgoz, S., Burd, H., Marasli, M. et al. (2023) 'Masonry buildings subjected to settlements: half-scale testing, detailed measurements, and insights into behaviour', *Eng. Struct*., 1 March, Vol. 278, p.115233.

Dalgic, K.D., Hendriks, M.A., Ilki, A. and Broere, W. (2019) 'A two-stage numerical analysis approach for the assessment of the settlement response of the pre-damaged historic Hoca Pasha Mosque', *Int. J. Archit. Herit*., Vol. 13, No. 5.

De Vent, I.A.E. (2011) 'Structural damage in masonry: developing diagnostic decision support'.

DIANA FEA (2023) *bv. Theory Manual (DIANA 10.8)*, Thijsseweg 11, 2629 JA Delft, The Netherlands.

Drougkas, A., Verstrynge, E., Szeker, P., Heirman, G., Bejarano-Urrego, L.E., Giardina, G. et al. (2020) 'Numerical modeling of a church nave wall subjected to differential settlements: soil-structure interaction, time-dependence and sensitivity analysis', *Int. J. Archit. Herit*., Vol. 14, No. 8, pp.1221–1238.

El Naggar, A., Youssef, M.A. and El Naggar, H. (2020) *Effect of Tunneling on Shallow Foundations*.

Ferlisi, S., Nicodemo, G. and Peduto, D. (2019) 'Numerical analysis of the behaviour of masonry buildings undergoing differential settlements', in *17th European Conference on Soil Mechanics and Geotechnical Engineering, Reykjavik*, International Society for Soil Mechanics and Geotechnical Engineering (ISSMGE), London, Vol. 10.

Ferlisi, S., Nicodemo, G., Peduto, D., Negulescu, C. and Grandjean, G. (2020) 'Deterministic and probabilistic analyses of the 3D response of masonry buildings to imposed settlement troughs', *Georisk*, Vol. 14, No. 4, pp.260–279.

Gazetas, G. (1991) 'Foundation vibrations', *Foundation Engineering Handbook*, pp.553–593, Springer.

Giardina, G., Marini, A., Hendriks, M.A.N., Rots, J.G., Rizzardini, F. and Giuriani, E. (2012) 'Experimental analysis of a masonry facade subject to tunnelling-induced settlement', *Eng. Struct.*, December, Vol. 45, pp.421–434.

Giardina, G., Rots, J. and Hendriks, M. (2013a) 'Modelling of settlement induced building damage'.

Giardina, G., Van de Graaf, A.V., Hendriks, M.A.N., Rots, J.G. and Marini, A. (2013b) 'Numerical analysis of a masonry facade subject to tunnelling-induced settlements', *Eng. Struct*., September, Vol. 54, pp.234–247.

Govindjee, S., Kay, G.J. and Simo, J.C. (1995) 'Anisotropic modelling and numerical simulation of brittle damage in concrete', *International Journal for Numerical Methods in Engineering*, Vol. 38, No. 21, pp.3611–3633.

Grünthal, G. (1998) *European Macroseismic Scale*, European Seismological Commission (ESC).

Jafari, S. (2021) *Material Characterisation of Existing Masonry: A Strategy to Determine Strength, Stiffness and Toughness Properties for Structural Analysis*, Delft University of Technology, TU Delft Applied Mechanics, Doctoral thesis, [online] https://repositorytudelftnl.

Korswagen, P.A. (2024) 'Quantifying the probability of light damage to masonry structures: an exploration of crack initiation and progression due to seismic vibrations on masonry buildings with existing damage'.

Korswagen, P.A., Longo, M., Meulman, E. and Rots, J.G. (2019) 'Crack initiation and propagation in unreinforced masonry specimens subjected to repeated in-plane loading during light damage', *Bulletin of Earthquake Engineering*, Vol. 17, pp.4651–4687.

Korswagen, P.A., Longo, M., Meulman, E. and van Hoogdalem, C. (2017) 'Damage sensitivity of Groningen masonry structures – experimental and computational studies', *Stream*, Vol. 1.

Korswagen, P.A., Longo, M., Prosperi, A., Rots, J.G. and Terwel, K.C. (2023) 'Modelling of damage in historical masonry façades subjected to a combination of ground settlement and vibrations', *International Conference on Structural Analysis of Historical Constructions*, Springer, pp.904–917.

Lin, H-D., Liao, H-C., Chen, S-L. and Chen, C-C. (2020) 'Interaction of excavation and adjacent building with different foundation types using 3D decoupled analysis method', *Geotechnics for Sustainable Infrastructure Development*, Springer, pp.321–327.

Longo, M., Sousamli, M., Korswagen, P.A., van Staalduinen, P. and Rots, J.G. (2021) 'Sub-structure-based 'three-tiered' finite element approach to soil-masonry-wall interaction for light seismic motion', *Eng. Struct*., 15 October, Vol. 245, p.112847.

Mylonakis, G., Nikolaou, S. and Gazetas, G. (2006) 'Footings under seismic loading: analysis and design issues with emphasis on bridge foundations', *Soil Dyn. Earthq. Eng*., September, Vol. 26, No. 9, pp.824–853.

NEHRP (2012) *NIST GCR 12-917-21 Soil-Structure Interaction for Building Structures*, National Institute of Standards and Technology, US Department of Commerce, Gaithersburg.

Netzel, H. and Kaalberg, F. (2000) 'Numerical damage risk assessment studies on adjacent buildings in Amsterdam', *ISRM International Symposium: ISRM*, p.ISRM-IS-2000-596.

Ninić, J., Gamra, A. and Ghiassi, B. (2024) 'Real-time assessment of tunnelling-induced damage to structures within the building information modelling framework', *Underground Space*, February, Vol. 14, pp.99–117.

NPR9998:2020en (2021) 'Assessment of structural safety of buildings in case of erection, reconstruction and disapproval – induced earthquakes – basis of design, actions and resistances'.

Prosperi, A., Korswagen, P.A., Korff, M., Schipper, R. and Rots, J.G. (2023a) 'Empirical fragility and ROC curves for masonry buildings subjected to settlements', *Journal of Building Engineering*, 1 June, Vol. 68, p.106094.

Prosperi, A., Longo, M., Korswagen, P.A., Korff, M. and Rots, J.G. (2023b) 'Sensitivity modelling with objective damage assessment of unreinforced masonry façades undergoing different subsidence settlement patterns', *Engineering Structures*, 1 July, Vol. 286, p.116113.

Prosperi, A., Longo, M., Korswagen, P.A., Korff, M. and Rots, J.G. (2024) '2D and 3D modelling strategies to reproduce the response of historical masonry buildings subjected to settlements', *International Journal of Architectural Heritage*, March, pp.1–17, DOI: 10.1080/15583058.2024.2325472.

Rots, J., Messali, F., Esposito, R., Jafari, S. and Mariani, V. (2016) 'Thematic keynote computational modelling of masonry with a view to Groningen induced seismicity', *Structural Analysis of Historical Constructions: Anamnesis, Diagnosis, Therapy, Controls: Proceedings of the 10th International Conference on Structural Analysis of Historical Constructions*, CRC Press, SAHC, Leuven, Belgium, 13–15 September, pp.227–238.

Schreppers, G., Garofano, A., Messali, F. and Rots, J. (2016) *DIANA Validation Report for Masonry Modelling*, DIANA FEA Report.

Son, M. and Cording, E.J. (2005) 'Estimation of building damage due to excavation-induced ground movements', *J. Geotech. Geoenviron.*, Vol. 131, No. 2, pp.162–177.

Sousamli, M. (2024) *Orthotropic Cyclic Continuum Constitutive Model for Masonry Structures and Comparative Studies*, PhD thesis, TU Delft.

Wikipedia (2010) Michiel1972, RM11994 Delft – Oude Delft 81.jpg.

Yiu, W., Burd, H. and Martin, C. (2017) 'Finite-element modelling for the assessment of tunnel-induced damage to a masonry building', *Geotechnique*, Vol. 67, No. 9, pp.780–794.